Experimental Investigation of Mechanical Properties of ASTM A992 Steel at Elevated Temperatures

JINWOO LEE, MOHAMMED A. MOROVAT, GUANYU HU, MICHAEL D. ENGELHARDT and ERIC M. TALEFF

ABSTRACT

This paper presents the results of a detailed experimental study into the mechanical properties of ASTM A992 structural steel at elevated temperatures. Critical testing issues, including temperature measurement, temperature control, and extensometer use, along with the testing equipment and procedures are briefly explained. Tensile steady-state temperature tests are conducted on samples of ASTM A992 steel at temperatures up to 1000 °C. Full stress-strain curves, representing steel coupons tested to fracture at elevated temperatures, are generated. Important mechanical properties such as yield stress, tensile strength, proportional limit, elastic modulus and elongation are obtained from the stress-strain curves. Results are compared with elevated-temperature properties specified by Eurocode 3 and by the AISC *Specification*. When defined as the stress at 2% total strain, the measured yield stress values agree reasonably well with the corresponding values from Eurocode 3 and the AISC *Specification*. However, for more conventional definitions of yield stress, such as the 0.2% offset yield stress, the agreement is poor. It is observed that the yield stress of steel at elevated temperatures up to about 600 °C is highly dependent on the manner in which yield stress is defined. The effects of displacement loading rates on steel strength and static yielding behavior are also investigated. It is shown that the displacement rate has a large impact on the steel strength at elevated temperatures, especially at temperatures higher than 600 °C. Further work is needed to fully characterize the time-dependent effects on the elevated-temperature stress-strain response of structural steel. Additionally, this paper presents results of Charpy V-Notch (CVN) tests on ASTM A992 steel at elevated temperatures.

Keywords: ASTM A992 steel, mechanical properties, retention factors, elevated temperatures, structural-fire engineering, fire safety.

INTRODUCTION

A key element in predicting the response of a steel structure to fire is knowledge of the elevated-temperature mechanical properties of structural steel. The properties of steel at high temperatures can be drastically different from those at room temperature. Computing the strength of steel members subjected to fire requires information on the yield stress, tensile strength, proportional limit and modulus of elasticity of steel at elevated temperatures. Advanced analysis methods, such as finite element analyses, require a more complete description of the elevated-temperature mechanical properties of steel, including data on the shape of the entire stress-strain curve as well as information on time-dependent effects such as strain rate effects and creep.

Considerable data on the elevated-temperature properties of structural steel have been published, including Harmathy and Stanzak (1970), Skinner (1972), United States Steel (1972), DeFalco (1974), Fujimoto et al. (1980, 1981), Cooke (1988), Kirby and Preston (1988), Lie (1992), Kelly and Sha (1999), Li et al. (2003), Luecke et al. (2005), Chen and Young (2006), Outinen (2006), Hu et al. (2009), and others. Nonetheless, significant gaps still exist in the database of elevated-temperature properties of structural steel. For example, ASTM A992 steel (see ASTM A992, 2011), the most common grade of structural steel used for wide-flange shapes in the United States, has not been widely examined at elevated temperatures. In addition, most previous publications on mechanical behavior of structural steel at high temperatures only report the initial portion of the stress-strain curve, leaving uncertainty on the elevated-temperature behavior of structural steel at large strains or the elevated-temperature ductility of structural steel. Further, elevated-temperature related properties such as static yielding behavior and the effect of loading rates have not yet been adequately studied. Further, the literature on high-temperature tension testing provides little information on the challenges in conducting such experiments. This is an important issue because testing techniques at elevated temperatures can have a significant effect on the test results.

Jinwoo Lee, Ph.D., P.E., S.E., Department of Civil and Architectural Engineering, Division of Nuclear Power Plant Design, Korea Electric Power Corporation E&C, Kyunggido, Republic of Korea. E-mail: jinwoo@kepco-enc.com

Mohammed A. Morovat, Ph.D. Candidate, Department of Civil, Architectural and Environmental Engineering, University of Texas at Austin, Austin, TX. E-mail: morovatma@mail.utexas.edu

Guanyu Hu, Ph.D., P.E., Engineer, 2H Offshore Engineering, Houston, TX. E-mail: huguanyu@gmail.com

Michael D. Engelhardt, Ph.D., P.E., Dewitt C. Greer Centennial Professor, Department of Civil, Architectural and Environmental Engineering, University of Texas at Austin, Austin, TX (corresponding). E-mail: mde@mail.utexas.edu

Eric M. Taleff, Ph.D., Professor, Department of Mechanical Engineering, University of Texas at Austin, Austin, TX. E-mail: taleff@mail.utexas.edu

Table 1. Chemical Composition of the Tested Specimens (Weight %)												
Coupon	**Source**	**Thickness**	**C**	**Cr**	**Mo**	**V**	**Ni**	**Mn**	**Si**	**P**	**S**	**Cu**
MA	W30×99; web	0.505 in.	0.081	0.09	0.034	0.065	0.11	1.41	0.21	0.019	0.022	0.39
MB	W30×99; web	0.525 in.	0.079	0.09	0.026	0.027	0.13	0.97	0.20	0.014	0.024	0.38
MC	W4×13; flange	0.345 in.	0.080	0.10	0.026	0.002	0.09	0.91	0.23	0.011	0.025	0.24

This paper presents results of a study on the elevated-temperature properties of ASTM A992 steel. Full-range stress-strain curves for this grade of steel at elevated temperatures up to 1000 °C are presented here, with a description of the testing equipment and procedures. The important mechanical properties of structural steel, including yield stress, tensile strength, proportional limit, elastic modulus and elongation, are obtained from the stress-strain curves. Results are compared with elevated-temperature properties specified by Eurocode 3 (2006) and by the AISC *Specification for Structural Steel Buildings*, hereafter referred to as the AISC *Specification* (2010). This paper also presents observations on the effect of cross-head displacement rate in tension tests at elevated temperatures. Test results for cross-head rates of 0.01 in./min and 0.1 in./min are presented. The static yielding behavior of ASTM A992 steel under elevated temperatures (300 to 800 °C) is also studied. Moreover, Charpy V-Notch (CVN) impact values are obtained to evaluate energy absorption capacity of ASTM A992 structural steel at elevated temperatures. Finally, this paper briefly discusses issues and difficulties that arise in performing and interpreting the results of such experiments. It should also be pointed out that a more complete account of this study is reported in a publication by Lee (2012).

EXPERIMENTAL PROGRAM

Equipment

Tension Tests at Elevated Temperatures

A 22-kip-capacity MTS 810 test frame equipped with MTS 647 water-cooled, hydraulic wedge grips was used to conduct the tension tests. The heating system consisted of the furnace, the furnace temperature controller and the data acquisition system for monitoring and recording furnace air temperature and coupon temperatures.

An MTS model 653 furnace (Figure 1a) was used as the heating device. The furnace generates heat using electrical coils and is separated into upper, middle and lower heating zones that can be individually controlled using an MTS model 409.83 temperature controller. Three thermocouples are located inside the furnace to measure the furnace air temperature.

Coupon temperatures were monitored and controlled using a separate data recording system as shown in Figure 1b. Three K-type thermocouple wires were used to measure the surface temperature at different locations along the gauge length of the coupon. The experimental set-up and a schematic diagram of the heating system used in the experimental program are shown in Figure 1b. An MTS model 632.54E-11 air-cooled high-temperature extensometer with 1-in. gauge length (with a limit strain of −5 to +10%) was used to measure strain. In order to capture the entire stress-strain relationship, throughout the course of the tests, the 1-in. gauge-length extensometer was reset when it approached the 10% limit. The procedure used for resetting the extensometer and for assembling the final stress-strain curves is described in Lee (2012).

Charpy Impact Tests at Elevated Temperatures

The Charpy V-Notch (CVN) tests were carried out at elevated temperatures by using a Tinius Olsen standard Charpy impact test machine. The heating system for the Charpy tests consisted of a small Thermolyne type 48000 bench-top muffle furnace, a temperature controller and a portable Oakton model 90600-40 thermometer.

Specimens

Tension Tests at Elevated Temperatures

In order to better assess the behavior of ASTM A992 steel at high temperatures considering the possible variability in steel material, specimens were cut from different wide-flange sections from different heats of steel. Specimens designated as MA and MB were cut from the web of W30×99 sections of two different heats of steel, and those designated as MC were cut from the flanges of a W4×13 section. Details of the dimensions of the specimens, in accordance with ASTM A370 (2012), are shown in Figure 2. The coupons were prepared so that their longitudinal dimension (18 in.) was along the rolling direction of the wide-flange sections. Moreover, though not specified by ASTM A370, the 18-in. length of the coupon was selected to create enough clearance between the furnace and the grips of the testing machine. The results of chemical analyses of the steels used in this research are presented in Table 1.

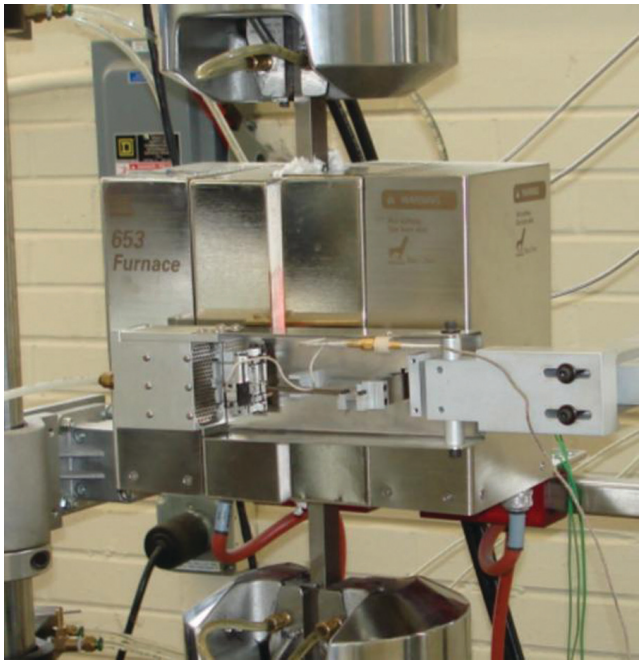

(a) Grips, wedges and furnace

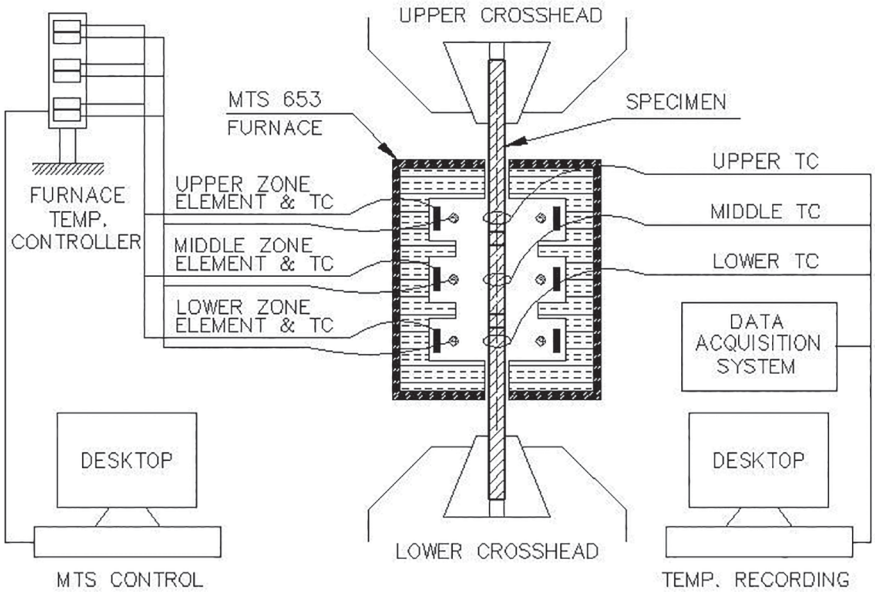

(b) Schematic diagram of heating system

Fig. 1. Test set-up consisting of the test machine and heating system.

Charpy Impact Tests at Elevated Temperatures

CVN test specimens were cut from material MB according to ASTM A370 (2012). Specimens used in the Charpy impact tests at elevated temperatures were bar-type specimens, 10 mm × 10 mm × 55 mm (0.39 in. × 0.39in. × 2.2 in.), with the V-notch machined in the center.

Procedure for Tension Tests at Elevated Temperatures

Overall Test Approach

High-temperature material tests on structural steel are usually conducted either under steady-state temperature conditions or under transient-state temperature conditions. In steady-state temperature tests, specimens are heated up to a specified temperature and then loaded to failure while maintaining the same temperature. During the initial heating process, the load is maintained at zero to allow free expansion of the specimen. The results of steady-state temperature tests are stress-strain curves at specified temperatures. Steady-state temperature tests can be carried out either as displacement or as load controlled. The resulting stress-strain curves can vary with the displacement or loading rate used in the test. In transient-state temperature tests, however, the specimens are loaded to a target stress level at ambient temperature and then heated up to failure while keeping the stress constant. Temperature and strain readings are recorded during these tests. After the test, thermal elongation is subtracted from the total strain. Finally, the results of a series of transient-state temperature tests conducted at different stress levels are converted into stress-strain curves at constant temperatures (Outinen, 2006). The resulting stress-strain curves can vary with the heating rate used in the test. A review of the literature and critical assessment of available data on high-temperature testing on structural steel indicates that for comparable loading and heating rates, the results from these two test methods are usually similar (Kirby and Preston, 1988; Outinen, 2006). Moreover, it can be interpreted that a primary reason for differences in the temperature-dependent stress-strain curves obtained from these two test methods is the influence of strain rate and creep at elevated temperatures. The influence of creep on tensile stress-strain behavior of structural steel at elevated temperatures and interpretation of such stress-strain data will be discussed briefly later in this paper.

The deciding factors on whether to choose steady-state or transient-state temperature test methods therefore come down to a matter of preference, type of equipment and how well the loading rate or temperature rate can be controlled. Based on the capabilities of the available test equipment, steady-state temperature tests, for temperatures from 20 to 1000 °C, were conducted in the investigation reported herein.

Besides being thermally steady-state, all tests were displacement-controlled, in which cross-head displacement rates were maintained at a constant value throughout a test. Specifically, two cross-head displacement rates were used: 0.01 in./min (slow test) for coupons made of MA, MB and MC materials, and 0.1 in./min (fast test) for coupons made of MA material.

Temperature Measurement and Control

Temperature measurement is a critical factor in elevated-temperature testing. Having a uniform temperature distribution over the gauge length of the steel coupon is crucial in order to accurately evaluate mechanical properties of steel at a specific temperature.

K-type thermocouple wires were used to measure the temperature at different locations along the gauge length of the coupon. Due to the fact that the thermocouple extension wire measures the temperature at the first contact point of its two dissimilar metals, this first contact point has to touch the surface of the steel coupon and maintain the initial position without moving during the test. Therefore, to have a reliable temperature measurement, thermocouple extension wires should be firmly attached to the surface of specimens. In addition, to be protected from radiation from the furnace

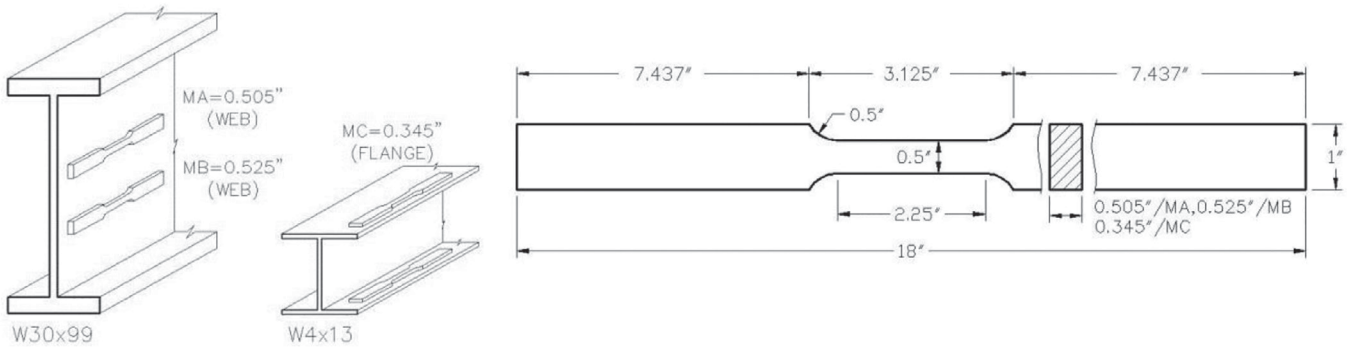

Fig. 2. Coupon specimens—designations and dimensions.

heating elements, the thermocouple wires were wrapped by Type 321 stainless steel tool wrap (Lee, 2012).

Note that considerable experience in elevated-temperature coupon testing was required before repeatable results were obtained. The investigators initially encountered significant difficulties in controlling the temperature of the coupons. It was found that a uniform air temperature in the three zones of the furnace resulted in a significant variation in steel temperature over the gauge length of the coupon. These problems were exacerbated as the coupon lengthened during testing and moved through different temperature zones in the furnace. Consequently, considerable trial-and-error experimentation was required before developing furnace control techniques that resulted in uniform steel temperatures over the height of the gauge section and throughout the duration of a test.

Load and Strain Measurement

The loading applied to the specimens was controlled and recorded by the load cell in the MTS test machine. The measured load was then used to calculate stress. The stress reported in this is engineering stress, which is equal to the measured load divided by the measured initial cross-sectional area of the coupon's reduced section.

Strains were measured using the 1-in. gauge-length MTS high-temperature extensometer described earlier. In addition to the extensometer, punch marks were placed on the specimen with initial 1-in. spacing. By measuring the initial distance between the punch marks and the final distance between punch marks (after fracture of the coupon), the strain at fracture—that is, the elongation—was determined. The initial and final distances between punch marks were measured when the coupon was at room temperature.

The strain recorded from the extensometer and the strain reported is engineering strain, based on the initial 1-in. gauge length of the extensometer. The extensometer contacts the coupon through ceramic rods, which extend outside of the furnace. Because the investigators were interested in capturing the full stress-strain curve up through fracture, which can occur at strains exceeding the 10% strain limit of the extensometer, a technique was developed for resetting the extensometer each time its 10% strain limit was reached and then reassembling the full stress-strain curves (Lee, 2012).

It should be emphasized here that testing steel coupons at elevated temperatures introduces a number of experimental difficulties that are not encountered in ambient-temperature testing. Specialized equipment is needed and considerable care and experience is required in temperature control, temperature measurement and strain measurement techniques. A more complete account of issues related to high-temperature testing of steel is reported in Lee (2012). The need for specialized equipment and specialized test techniques, and the need for considerable experience, have likely contributed to the paucity of elevated-temperature stress-strain data for structural steel.

Testing Procedure for Charpy Impact Tests at Elevated Temperatures

To perform CVN tests at elevated temperatures, CVN specimens were first heated up to the target temperatures in an electric furnace, as described previously. In general, the target temperatures were achieved within 20 min and were maintained thereafter for about an hour. Next, heated specimens were positioned in the Charpy impact machine to complete the tests. It is important to note that there is a loss in the specimens' temperature as they are taken out of the furnace and set down in the Charpy impact machine. To compensate for such temperature losses, the specimens were initially heated to temperatures about 5% more than the target temperatures.

EXPERIMENTAL RESULTS

In this section, experimental data are presented in the form of stress-strain curves for tension tests at elevated temperatures. Effects of different parameters such as variability in the steel material, elevated temperature, cross-head displacement rate and static yielding phenomenon on the tensile stress-strain behavior are illustrated and discussed. Data from the Charpy impact tests at elevated temperatures are also provided.

Specimens Following Tests at Elevated Temperatures

The necking and elongation patterns of representative coupons from elevated-temperature tension tests on material MA are shown in Figure 3. It can be observed that at temperatures of 800 and 900 °C, the necking shows a trend of distributing more along the length of the coupon's reduced section. Coupons tested at 300 °C exhibited a characteristic blue color after testing. Similarly, coupons tested at very high temperatures, above about 700 °C, exhibited a black and very rough surface appearance. Fracture surfaces in coupons tested at lower temperatures exhibited sharp corners at failure locations.

The fracture surfaces and deformation patterns of the specimens from elevated-temperature Charpy impact tests are shown in Figure 4. As can be seen from this figure, at temperatures above 700 °C, specimens bent but did not break at the location of the notches.

Stress-Strain Curves

Effect of Elevated Temperature

To illustrate the effect of elevated temperatures on tensile properties of ASTM A992 steel, stress-strain curves are

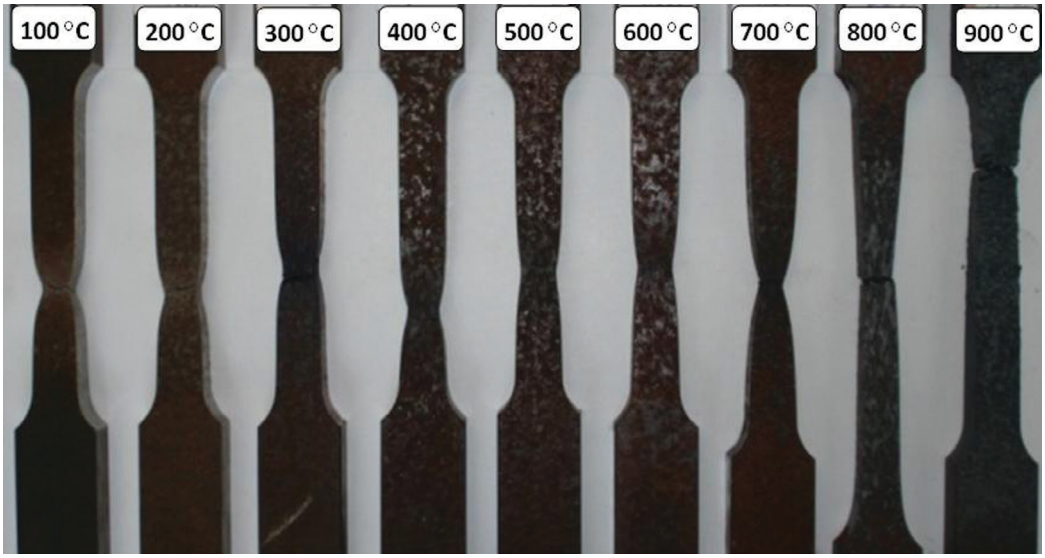

Fig. 3. Material MA coupons after elevated-temperature tests.

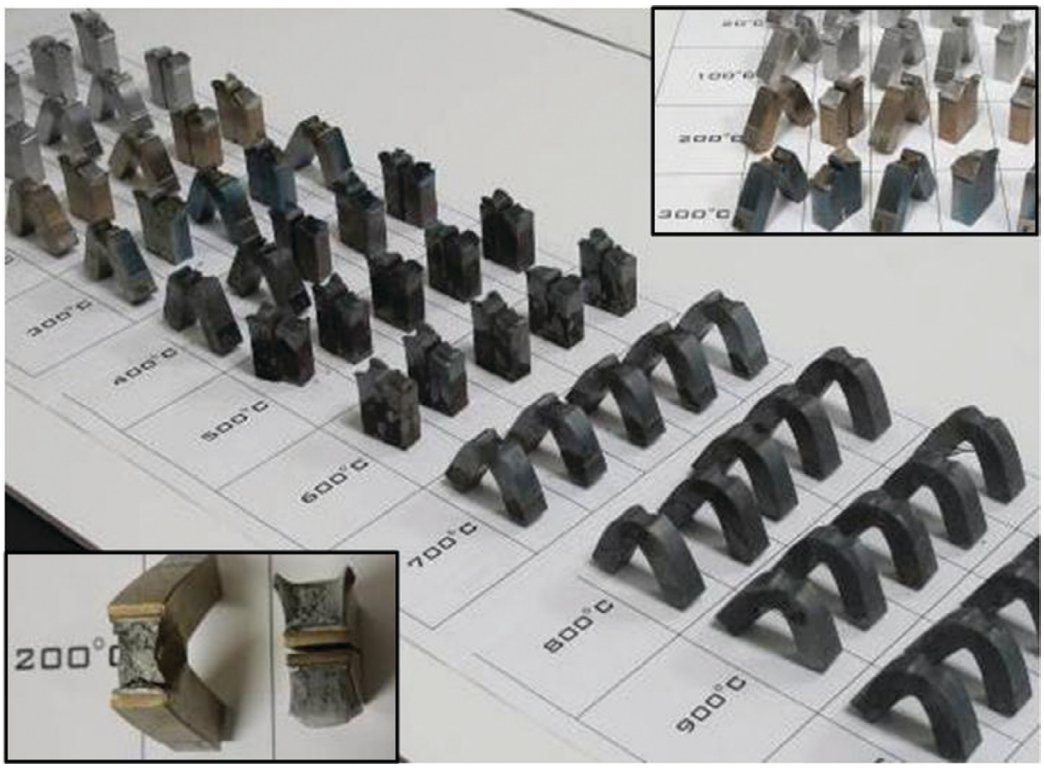

Fig. 4. Material MB specimens after Charpy impact tests at elevated temperatures.

presented for different designations of steel materials; MA, MB and MC in Figures 5, 6 and 7, respectively. In these figures, stress-strain curves are plotted up to 80% strain, which includes strains from the start of loading to the fracture of the coupons at different temperatures, except for materials MA and MB at 800 °C, for which the strains at fracture are 128% and 120%, respectively. All stress-strain curves presented in Figures 5, 6 and 7 are for a cross-head displacement rate of 0.01 in./min. As illustrated in Figures 5a, 6a and 7a, for each material, the tensile strength increases compared to the corresponding one at room temperature, at temperatures of 200 and 300 °C. At higher temperatures, progressive loss in the tensile strength can be clearly observed. Another important property, ductility, as measured by the final elongation of the coupons, exhibits a small reduction up to 500 °C, then increases in the range of 600 to 800 °C and then reduces again at 900 °C. On the other hand, ductility, as measured by the strain at which the tensile strength is developed, shows a dramatic decrease with increasing temperature from 400 to 700 °C. Furthermore, Figures 5b, 6b and 7b plot the initial parts of the stress-strain curves up to 0.5% strain for each material. These figures clearly show that the yield stress and modulus of elasticity decrease with temperature.

As observed in previous tension tests reported in the literature, these data show that the fundamental shape of the stress-strain curve changes as temperature increases. At 400 °C and above, the steel no longer exhibits a well-defined yield plateau and shows significant nonlinearity at low levels of stress and strain. Likewise, as described earlier, the strain corresponding to the maximum engineering stress (tensile

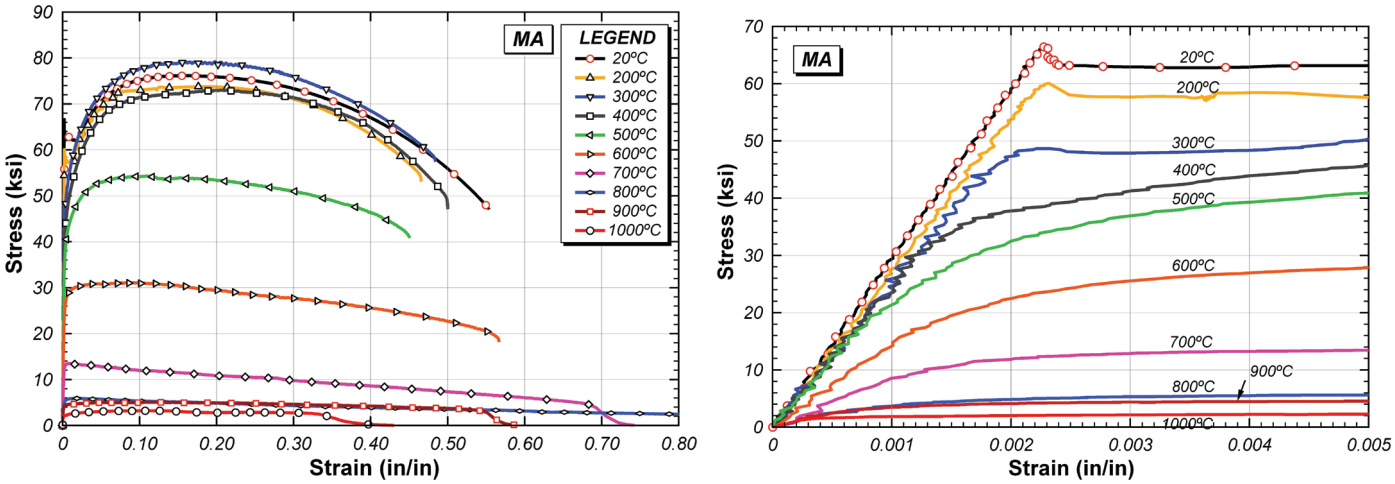

(a) Full-range stress-strain curves *(b) Initial portion of stress-strain curves*

Fig. 5. Stress-strain curves for material MA at elevated temperatures.

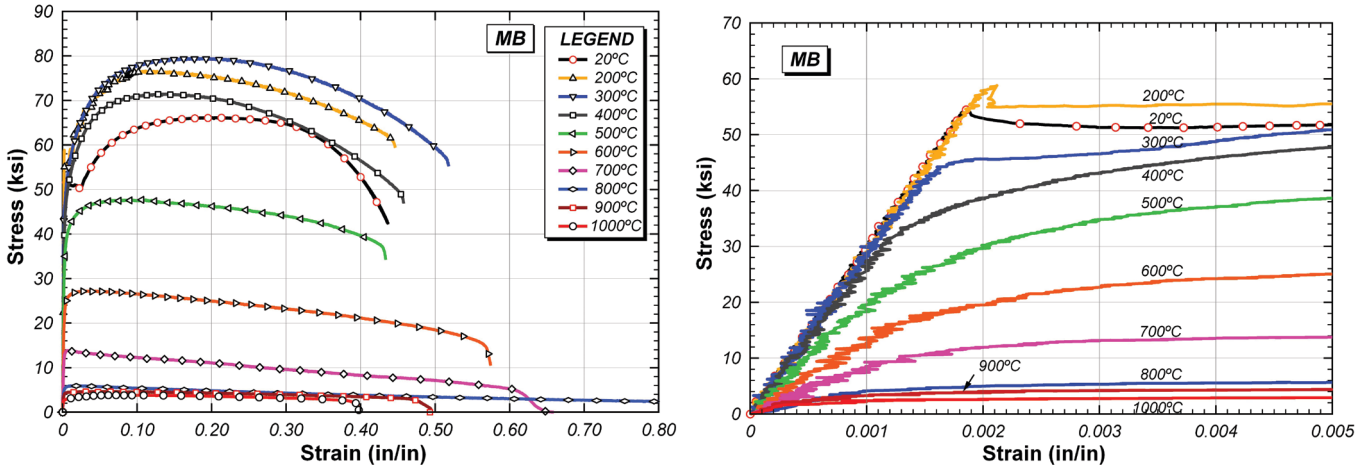

(a) Full-range stress-strain curves *(b) Initial portion of stress-strain curves*

Fig. 6. Stress-strain curves for material MB at elevated temperatures.

strength) decreases rapidly as temperature increases, and the stress-strain curve subsequently shows a long, gradual decline.

At ambient temperature, the initial portion of the stress-strain curve is often modeled using a simple elastic–perfectly plastic approximation, in which the response is linear-elastic up to yield and then follows a plateau. Simple elastic–perfectly plastic stress-strain models may be less appropriate at elevated temperatures due to early nonlinearity in stress-strain curves, as seen in Figures 5, 6 and 7. This early nonlinearity may be particularly significant when considering stability phenomena, wherein tangent stiffness is a critical material property.

Effect of Material Variability

Figure 8 illustrates the effect of material variability by presenting stress-strain curves at specific temperatures for materials designated as MA, MB and MC. Stress-strain curves presented in Figure 8 are for a cross-head displacement rate of 0.01 in./min. As is clear from this figure, there is appreciable difference in material stress-strain response among these three materials, which are all classified as ASTM A992 steel. More specifically, it can be observed from this figure that materials MA and MB, both from the web of W30×99 sections of different heats, show similar stress-strain behaviors at elevated temperatures. The difference in behavior of materials MA and MB at room temperature may be attributed to the difference in chemistry, especially in terms of molybdenum and manganese contents. It can also be observed that the stress-strain curves of material MC, which is from the flange of a W4×13 section, are very different from those of materials MA and MB at elevated temperatures. Of particular interest is the comparison among these three materials at 200 °C, where very large strain hardening and a very large increase in tensile strength are seen in the stress-strain behavior of material MC. At first, this behavior was suspected to be experimental error. However, several coupons of MC material were tested at 200 °C, and this same behavior was consistently observed. These observations suggest that there may be considerable variability in stress-strain response for a particular grade of steel, and this variability should be considered in any attempt at developing general stress-strain material models for structural steel at elevated temperatures.

Some additional interesting trends can be observed from these data. For example, a phenomenon in which the stress-strain curves are not smooth in the strain hardening range, but rather exhibited a number of sudden stress jumps, can be observed at 200 °C for all materials (Figure 8b). At first, this was believed to be slipping of the extensometer. However, this effect was observed repeatedly in tests at 200 °C and thus did not appear to be experimental error. A review of the literature suggests this may be a metallurgical phenomenon known as the Portevin-LeChatelier effect (Dieter, 1986). In addition, the stress-strain curves at 1000 °C (Figure 8j) show multiple peaks rather than just one, a characteristic that cannot be seen in the stress-strain behavior at any other temperature considered in this test program. This phenomenon, which is known as dynamic recrystallization, has been reported in the literature on properties of metals at elevated temperatures (Humphreys and Hatherly, 2004).

Effect of Cross-Head Displacement Rate

Loading rate can have a significant effect on the measured stress-strain curves of structural steel, and this effect appears to be more pronounced at elevated temperatures. To address the influence of loading rates on tensile test results at elevated temperatures, the tensile tests were carried out with two different cross-head displacement rates. Figure 9 shows the comparison of stress-strain curves for cross-head

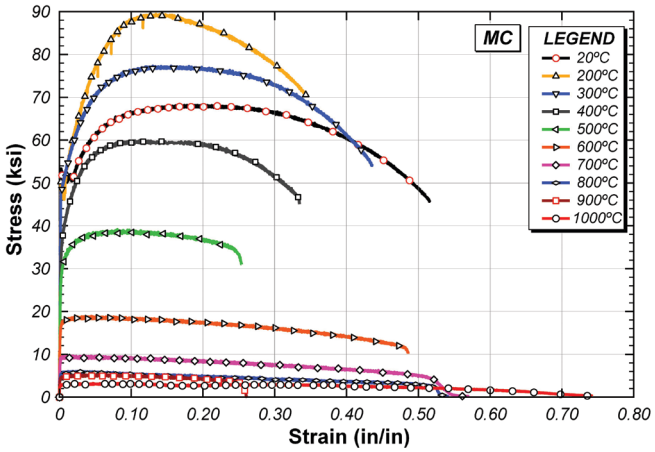

(a) Full-range stress-strain curves

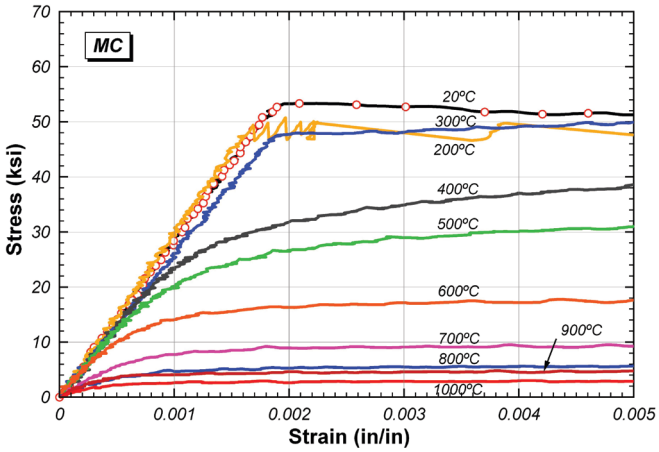

(b) Initial portion of stress-strain curves

Fig. 7. Stress-strain curves for material MC at elevated temperatures.

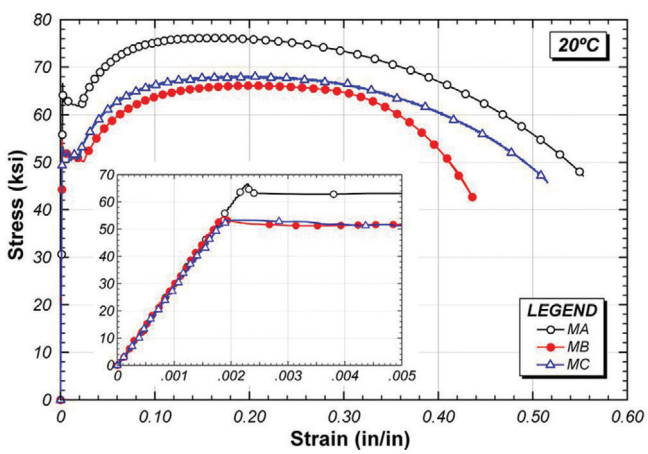

(a) Room temperature

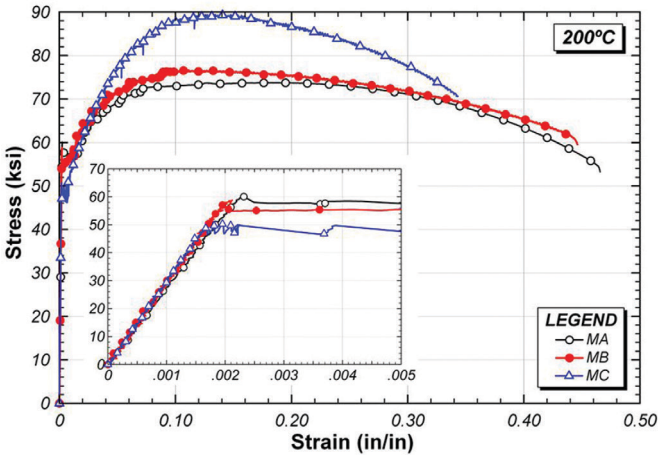

(b) 200 °C

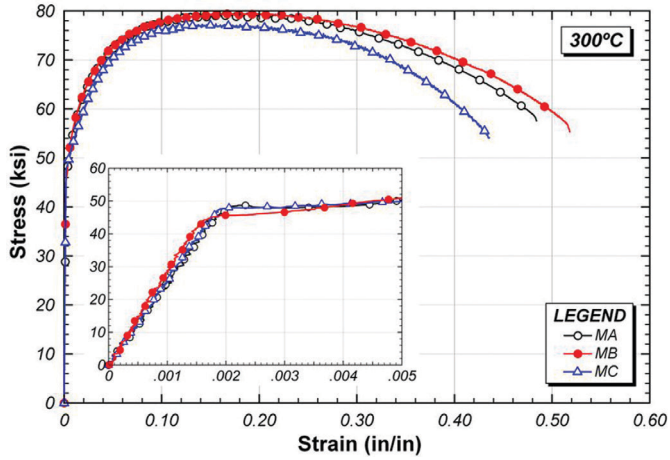

(c) 300 °C

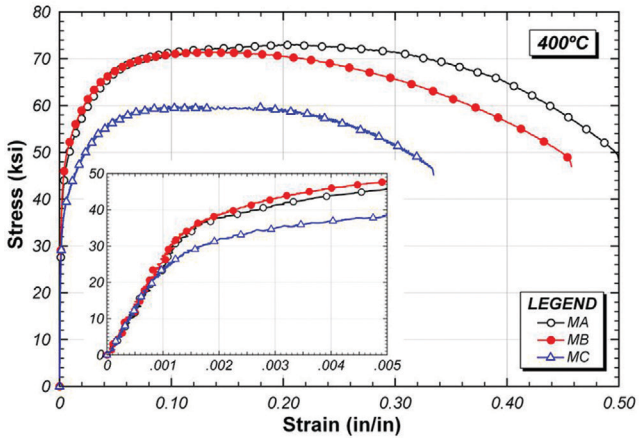

(d) 400 °C

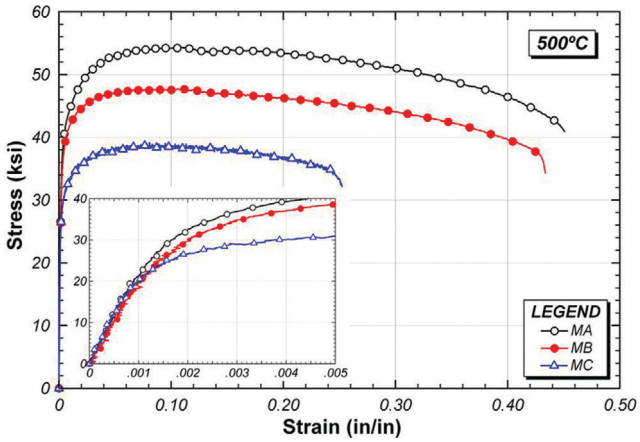

(e) 500 °C

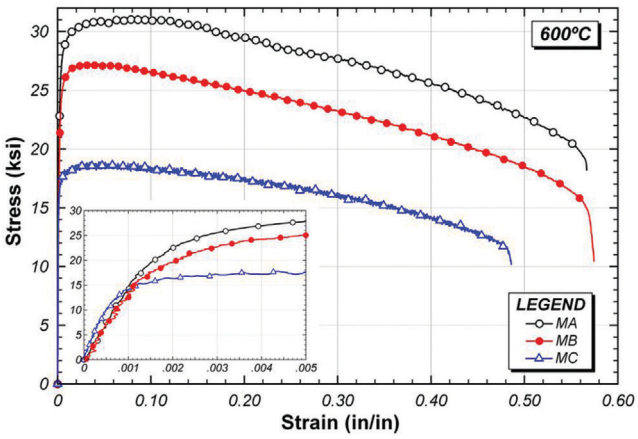

(f) 600 °C

Fig. 8. Comparison of elevated-temperature stress-strain curves for three different ASTM A992 materials.
(continued on next page)

displacement rates of 0.01 in./min and 0.1 in./min at each temperature for temperatures up to 900 °C (for the material designated as MA. Figure 9j plots and compares the full stress-strain curves measured using the two displacement rates for the entire range of tested temperatures. Similarly, the initial portions of the stress-stain curves are plotted up to 2% strain in Figure 10. As can be seen from these figures, at lower temperatures up to 400 °C, there is little difference in the stress-strain curves from the two different displacement rates. Some of the differences observed in the shape of stress-strain curves at these temperatures are likely related to the inherent material variability from one coupon specimen to another. It is at 500 °C and above that the differences between the two cross-head displacement rates become more significant. For instance, at temperatures higher than 500 °C, the displacement rate of 0.1 in./min results in yield and tensile strengths 30 to 40% higher than those obtained at 0.01 in./min. These data suggest the importance of controlling and reporting loading rates in elevated-temperature tests on structural steel materials, members and connections, and in considering rate effects in overall analysis and design of steel structures for fire conditions.

Effect of Static Yielding

In ambient temperature testing, static yield stress values are often measured in coupon tests to provide a zero-strain rate evaluation of yield stress. Static yield values are useful in research for comparing member and material tests at comparable strain rates (SSRC, 1987) and are useful in the development of design rules that properly account for loading-rate effects (Beedle and Tall, 1960). Static yield stress values at ambient temperature are obtained by stopping the machine cross-heads and holding the cross-heads at a fixed displacement for 3 to 5 min and then reading the value of stress. In the elevated temperature tests reported here, static yielding was examined by suspending cross-head movement during tension tests for periods of either 30 min or 3 min and then measuring the subsequent stress relaxation. These

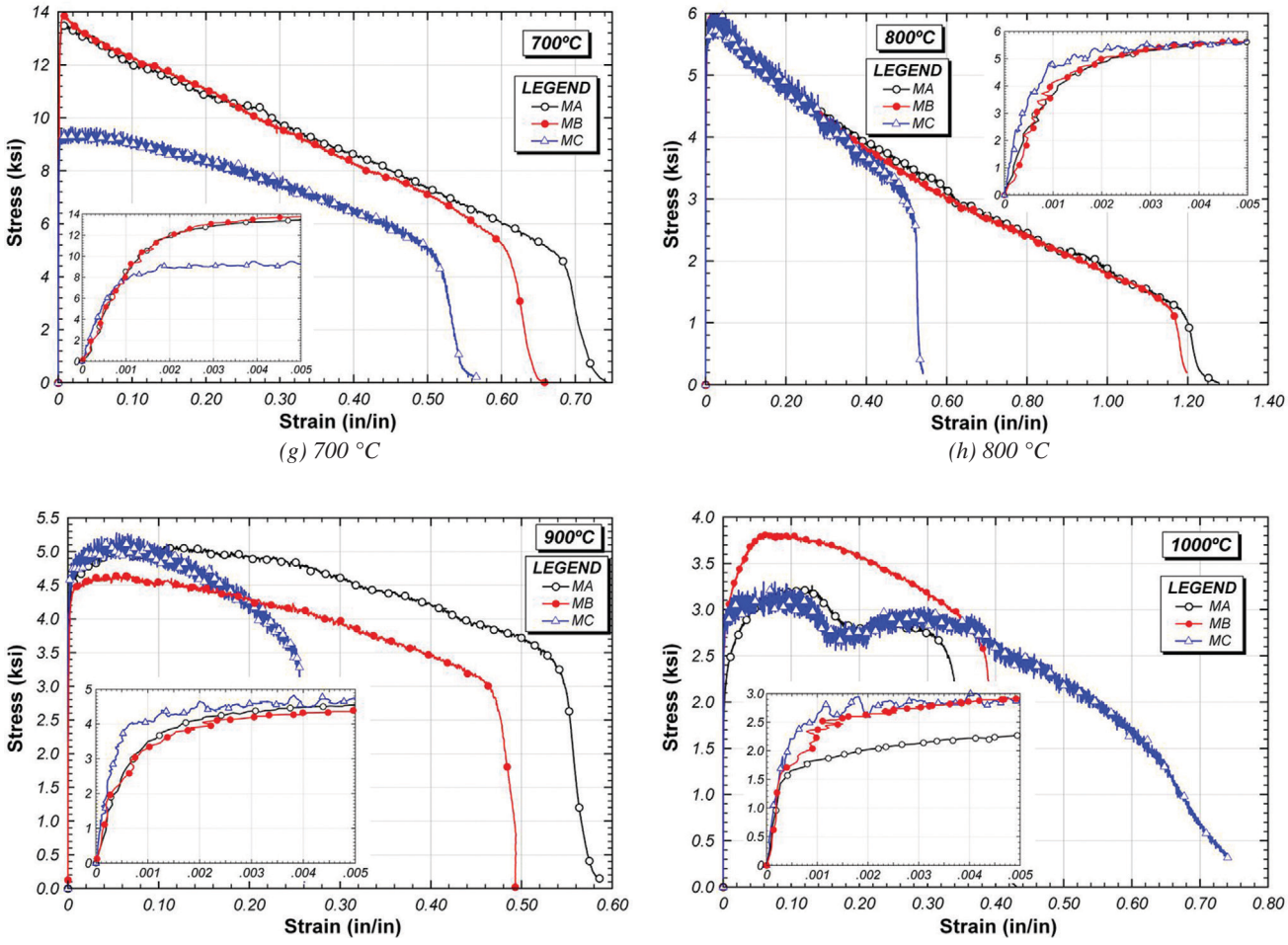

(g) 700 °C (h) 800 °C

(i) 900 °C (j) 1000 °C

Fig. 8. Comparison of elevated-temperature stress-strain curves for three different ASTM A992 materials.
(continued from previous page)

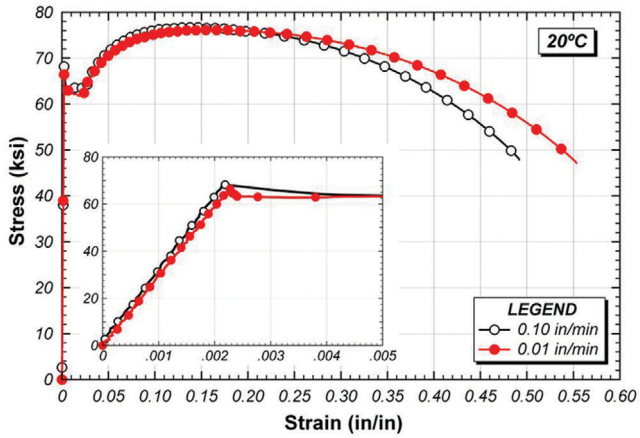

(a) Room temperature

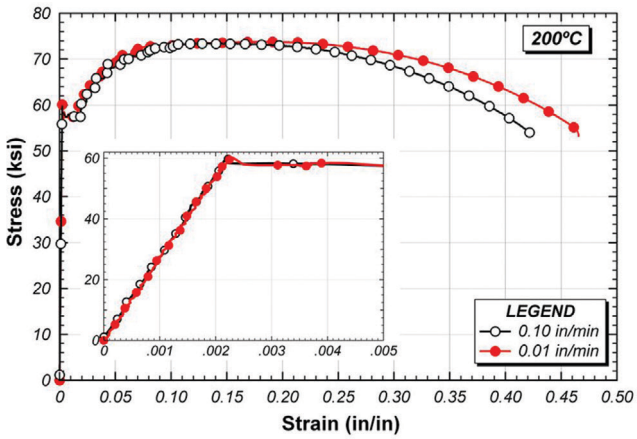

(b) 200 °C

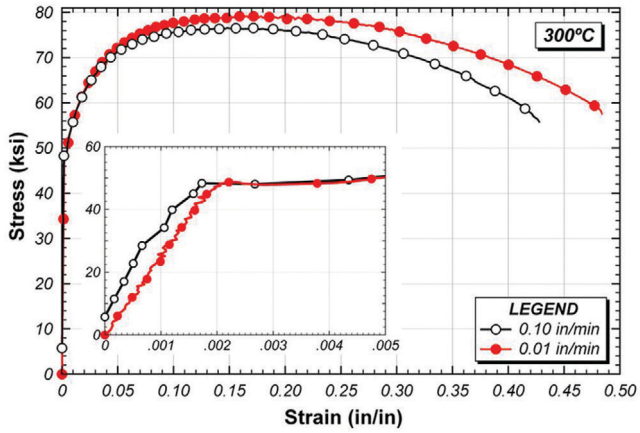

(c) 300 °C

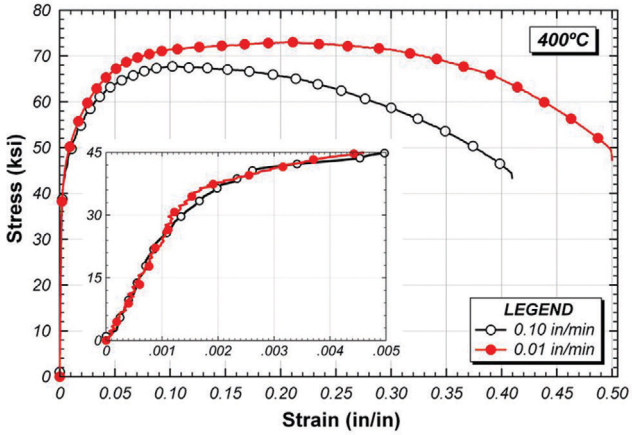

(d) 400 °C

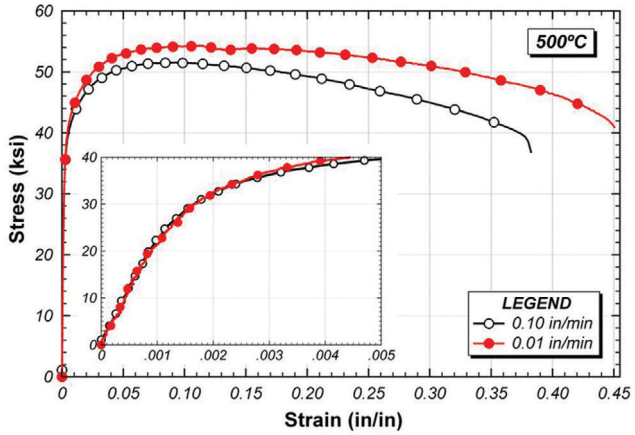

(e) 500 °C

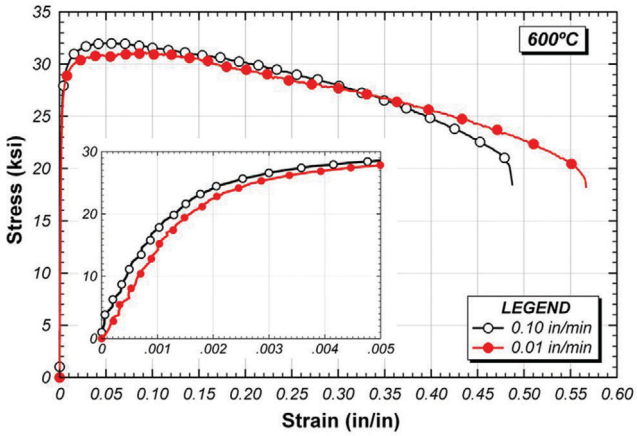

(f) 600 °C

Fig. 9. Comparison of elevated-temperature stress-strain curves for different cross-head displacement rates.

(continued on next page)

static yielding tests were conducted during the slow tests (0.01 in./min) on material MA at different temperatures. The resulting stress-strain curves are shown in Figure 11. Compared with dynamic yielding, static yielding produced significantly lower values of steel strength at high temperatures. For example, at 800 °C, the steel strength almost dropped to zero after a 30-min cross-head hold. The significant difference between static and dynamic yielding reflects the influence of creep and relaxation at high temperatures. Interestingly, at 300 °C, such static yielding behavior tests increased the tensile strength of the coupon, which may be due to strain aging phenomenon at that temperature. The data in Figure 11 further illustrate the importance of rate effects on the effective strength of steel at elevated temperatures and the influence of creep. These factors are often neglected in describing the high-temperature stress-strain response of structural steel but appear to be very important phenomena that merit further investigation. The effect of creep on tensile stress-strain behavior of structural steel at elevated temperatures and interpretation of such stress-strain data will be discussed in more detail later in this paper.

Charpy Impact Tests

Charpy V-Notch impact tests were conducted on samples of steel from material MB that were subjected to elevated temperatures up to 1,000 °C. Results of these tests are listed in Table 2 as impact energies in foot-pounds (ft-lb). As can be seen from Table 2, the results show a significant reduction in CVN values with temperature for temperatures up to 600 °C and then a sharp increase at 700 °C. At temperatures higher than 700 °C, CVN values again start to decrease almost linearly with temperature.

ANALYSIS OF EXPERIMENTAL DATA

In this section, analyses and further discussions of the experimental data are provided along with comparisons of key mechanical properties derived from the stress-strain curves

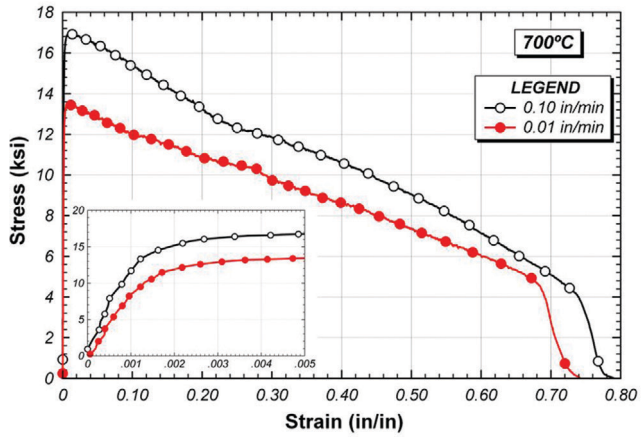

(g) 700 °C

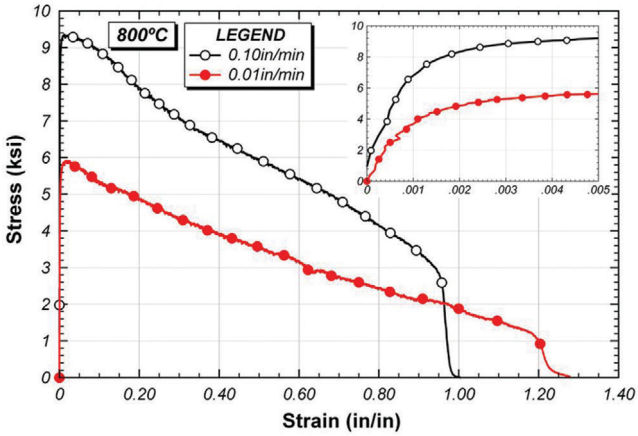

(h) 800 °C

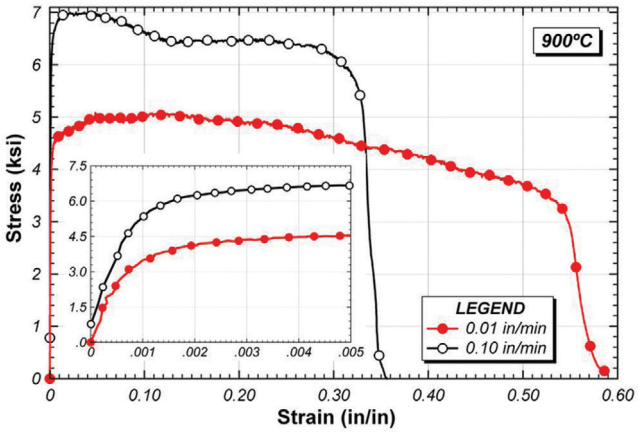

(i) 900 °C

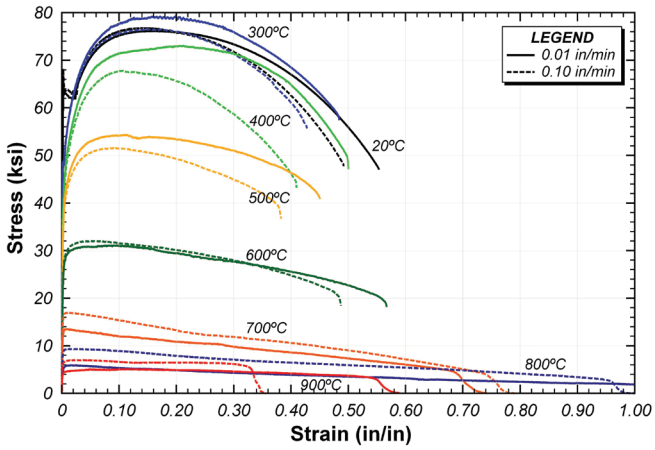

(j) Full stress-strain curves at different temperatures

Fig. 9. Comparison of elevated-temperature stress-strain curves for different cross-head displacement rates.
(continued from previous page)

Table 2. CVN Impact Energy for ASTM A992 Steel at Elevated Temperatures (ft-lb)										
Temperature (°C)	**20**	**200**	**300**	**400**	**500**	**600**	**700**	**800**	**900**	**1000**
CVN value	238	233	209	143	69	59	183	134	103	64

at elevated temperatures. These properties include the yield stress, tensile strength, proportional limit, elastic modulus and total elongation. Data on selected properties are also compared with the predictions from Eurocode 3 (2006) and the AISC *Specification* (2010).

General Observations

As can be observed from Figures 5, 6 and 7, the stress-strain behavior of ASTM A992 steel undergoes significant changes as temperature increases. In general terms, the steel loses strength and stiffness with increase in temperature. More specifically, at elevated temperatures, both the yield stress and the modulus of elasticity are reduced from their room-temperature values. Except for low temperatures, the tensile strength also reduces with temperature. In addition to the reduction in yield stress, tensile strength and modulus of elasticity, the shape of the stress-strain curve at high temperatures is fundamentally different from the corresponding one at ambient temperature. At high temperatures, the stress-strain curve does not exhibit a well-defined yield plateau and becomes highly nonlinear at low levels of stress. In other words, at elevated temperatures, the proportional limit occurs at a stress less than the yield stress. It should be emphasized that the greater nonlinearity exhibited by the stress-strain curves at high temperatures can have a significant influence on member behaviors governed by stability modes of failure, where stiffness is a critical material property.

Yield Stress

At temperatures above approximately 300 to 400 °C, the measured stress-strain curves do not exhibit a well-defined yield plateau. Consequently, defining yield stress becomes more subjective at elevated temperatures than at ambient temperature. For metals that do not exhibit a yield plateau, the 0.2% offset yield stress definition is widely used and is specified by ASTM E21 (ASTM, 2009) for defining the yield stress at elevated temperatures. With this method, yield stress is defined as the stress at the intersection of the stress-strain curve and the proportional line offset by 0.2% strain. This definition of yield stress is also presented graphically in Figure 12. Within the literature on elevated-temperature properties of structural steel, various definitions of yield stress have been used. In addition to the conventional 0.2% offset definition, the yield stress has also been defined as the stress corresponding to 0.5% total strain and as the stress corresponding to 2% total strain, as well as other definitions. These alternate definitions are also illustrated in Figure 12. Both Eurocode 3 (2006) and the AISC *Specification* (2010) have adopted the 2% total strain definition for the yield stress of structural steel at elevated temperatures. It is important to note that because this definition is not a standard definition for yield stress, the yield stress corresponding to the 2% total strain is called "effective yield stress" in Eurocode 3. Figure 13 shows the initial portion of a stress-strain curve from this test program for 400 °C and a cross-head displacement rate of 0.01 in./min. The values of yield stress are shown for

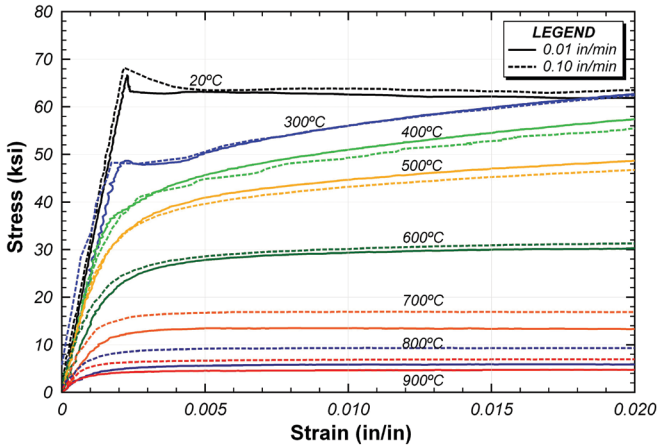

Fig. 10. Cross-head displacement-rate effects at elevated temperatures—stress-strain curves up to 2% strain.

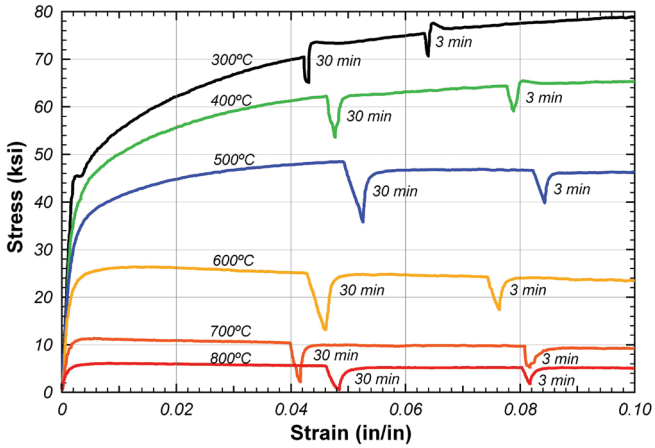

Fig. 11. Static yield phenomenon at elevated temperatures for ASTM A992 steel.

the three definitions of yield stress: 43.8 ksi for 0.2% offset strain, 45.8 ksi for 0.5% total strain and 57.5 ksi for 2% total strain definition. It is clear that the choice of the definition of yield stress can have a very large impact on the resulting value of yield stress.

Yield stress retention factors based on the data collected in this research are plotted in Figure 14. The yield stress retention factor is defined as the yield stress at a specific temperature (using stress-strain curves at 0.01 in./min cross-head displacement rate) divided by the yield stress at ambient temperature. The retention factors for yield stress based on the 0.2% offset, 0.5% total strain and 2% total strain definitions are compared with retention factors from Eurocode 3 (2006) and from the AISC *Specification* (2010) in Figure 14. Note that Eurocode 3 and the AISC *Specification* use the same retention factors for yield stress and are, therefore, plotted as a single line. As can clearly be seen from Figures 14a and 14b, for temperatures in the range of 100 to 500 °C, the yield stress retention factors from tests, based on the 0.2% offset and 0.5% total strain definitions, are significantly lower than the corresponding values specified by Eurocode 3 and the AISC *Specification*. To the contrary, Figure 14c shows a good agreement between retention factors from test data and those predicted by the codes, when the retention factors for the test data are based on the 2% total strain definition of yield stress. Similar observations can be made from Figures 14d, 14e and 14f, where yield stress retention factors are presented and compared with code predictions for materials MA, MB and MC, respectively. From these figures, it can be seen that the values of yield stress from the test data are fairly close to one another for the 0.2% offset and 0.5% total strain definitions. Further, above about 600 °C, all three definitions of yield stress give similar values. However, below 600 °C, the yield stress based on the 2% total strain definition is significantly higher than the yield stress values based on the other two definitions.

As is clear from Figure 14, the yield stress of steel at elevated temperatures up to about 600 °C is highly dependent on the manner in which it is defined. Based on Twilt and Both (1991), it appears that the yield stress retention factors for structural steel at elevated temperatures used in Eurocode 3 (2006) were adopted from British Steel Corporation data (Kirby and Preston, 1988). However, little was found in the literature to support this definition of yield stress for structural-fire engineering design of steel structures. It seems that the most appropriate definition for yield stress of steel at elevated temperatures ultimately lies in how these values are used in design formulas, and further investigation and discussion of this issue appears justified. The design implications of different definitions for the yield stress will be discussed in more detail later in this paper.

Finally, for reference, the yield stress values evaluated using different definitions for each steel material at elevated temperatures are presented in Table 3. The yield stress data reported in Table 3 are based on tension tests conducted under the slow rate condition of 0.01 in./min.

Tensile Strength

The retention factors for tensile strength, obtained for all steel materials tested in this program, are compared with the corresponding values in Eurocode 3 (2006) and AISC *Specification* (2010) in Figure 15. In Figure 15a, the tensile strength retention factor is defined as the tensile strength measured at a specific temperature (using stress-strain curves at 0.01 in./min cross-head displacement rate) divided by the yield stress measured at ambient temperature. The data are presented in this manner because this is how the tensile strength retention factor is defined in both Eurocode 3 (2006) and the AISC *Specification* (2010). For temperatures at and above 400 °C, both Eurocode 3 and the AISC *Specification* take the elevated-temperature tensile strength

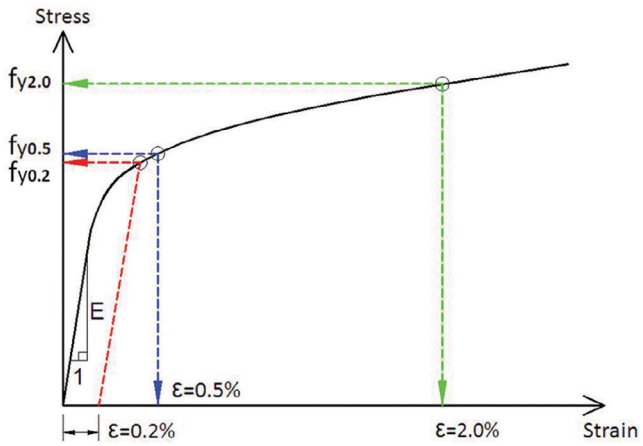

Fig. 12. Different definitions of yield stress.

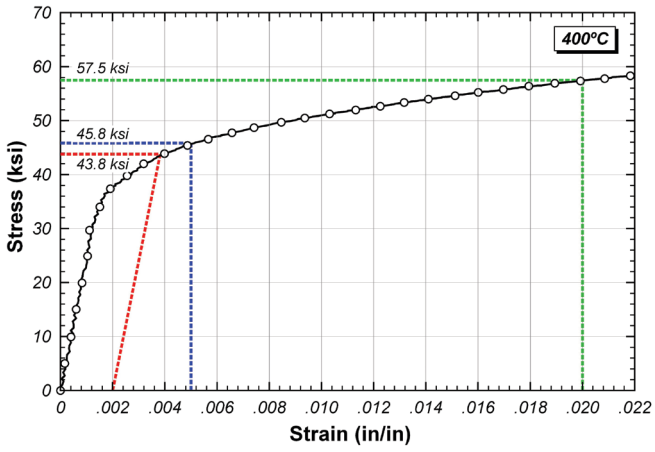

Fig. 13. Yield stress values for test at 400 °C.

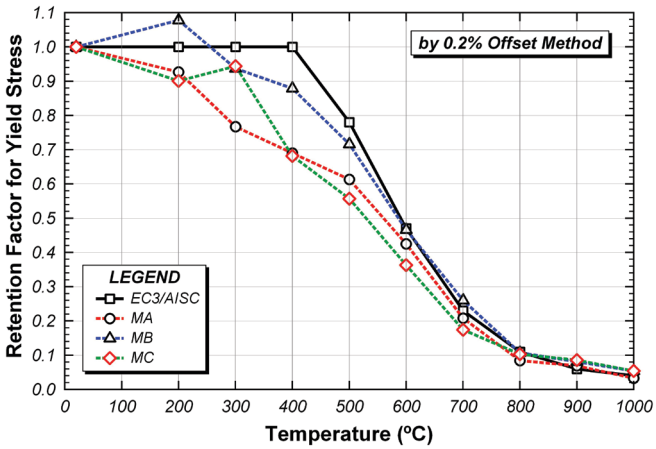

(a) 0.2% offset definition

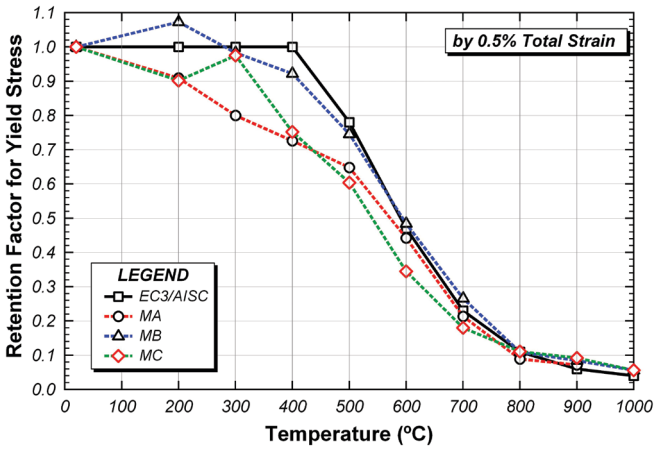

(b) 0.5% total strain definition

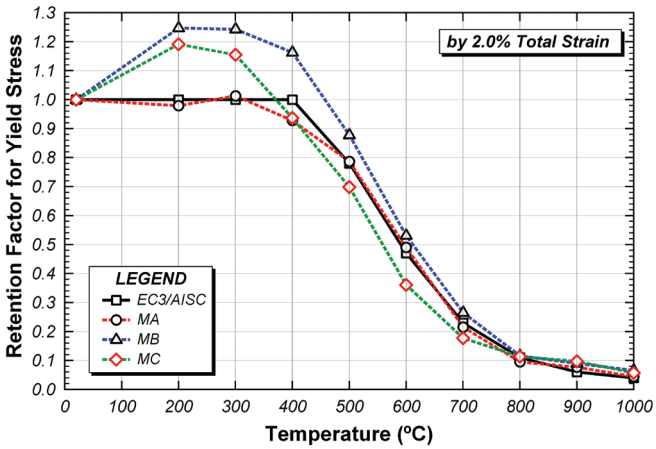

(c) 2% total strain definition

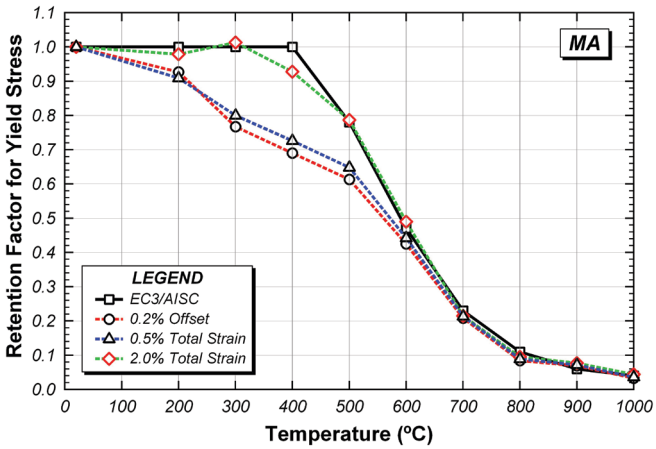

(d) Material MA: different yield stress definitions

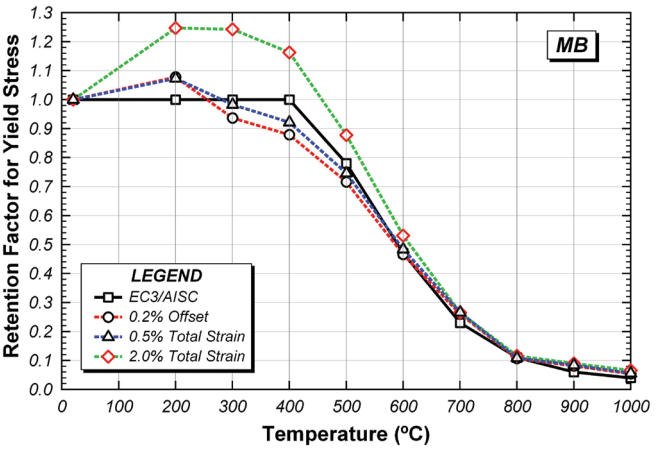

(e) Material MB: different yield stress definitions

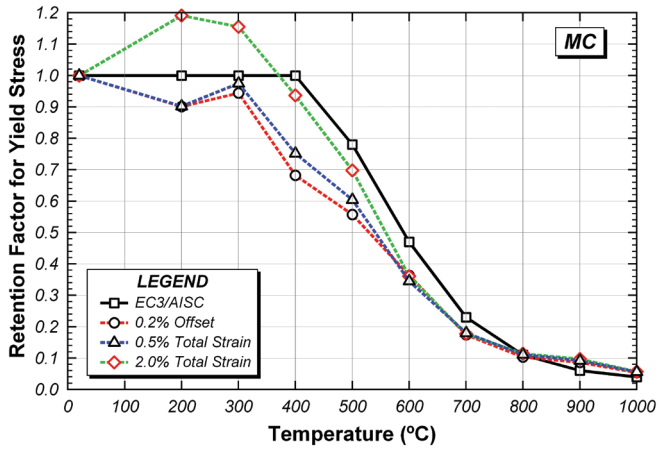

(f) Material MC: different yield stress definitions

Fig. 14. Yield stress retention factors.

Table 3. Yield Stress Values for ASTM A992 Steel at Elevated Temperatures (ksi)											
Temperature (°C)		20	200	300	400	500	600	700	800	900	1000
MA	0.2% offset	63.1	58.5	48.4	43.5	38.7	26.8	13.1	5.3	4.4	2.1
	0.5% total strain	63.2	57.4	50.5	45.8	41.0	27.9	13.5	5.6	4.6	2.3
	2.0% total strain	61.9	60.6	62.8	57.5	48.7	30.3	13.3	5.9	4.7	2.7
MB	0.2% offset	51.4	55.4	48.2	45.2	36.8	24.0	13.3	5.5	4.1	2.8
	0.5% total strain	51.7	55.5	50.8	47.7	38.6	25.1	13.8	5.7	4.4	2.9
	2.0% total strain	50.9	63.4	63.2	59.2	44.6	27.0	13.5	5.9	4.6	3.4
MC	0.2% offset	51.8	46.7	48.9	35.4	28.8	16.8	9.0	5.3	4.5	2.8
	0.5% total strain	51.3	46.3	50.0	38.6	31.0	17.7	9.2	5.7	4.7	2.9
	2.0% total strain	51.6	61.4	59.6	48.3	36.0	18.6	9.2	5.9	5.0	3.0

equal to the elevated-temperature yield stress, or elevated-temperature effective yield stress as defined by Eurocode 3.

Figure 15b shows the tensile strength retention factors from the tests, where the retention factor is defined as tensile strength measured at a specific temperature divided by the tensile strength measured at ambient temperature (using stress-strain curves at 0.01 in./min cross-head displacement rate). This seems to be a more conventional definition of tensile strength retention factor. For reference, the tensile strength values obtained for each steel material at elevated temperatures are shown in Table 4. Comparing the elevated-temperature tensile strength values listed in Table 4 with the elevated-temperature yield stress values based on the 2% total strain definition listed in Table 3, it can be seen that the tensile strength generally exceeds the yield strength for temperatures up through and including 500 °C. For 600 °C and above, the measured tensile strength and yield strength values are essentially the same.

Elastic Modulus

The elastic modulus was determined by measuring the slope of the initial linear portion of the stress-strain curves for tests conducted at a cross-head displacement rate of 0.01 in./min. Strains were measured in the tension coupon tests using a nonaveraging type extensometer; that is, strains were measured on only one side of the coupon. Consequently, errors at small strain levels can occur due to bending of the coupon resulting in errors in the measured strain. As such, the elastic modulus values derived from the stress-strain curves may be subject to some error. Nonetheless, the elastic modulus data were still examined for general trends.

The variation of elastic modulus with temperature is plotted in Figure 16 for all steel materials tested in this program. Retention factors for elastic modulus are plotted in Figure 17, where the retention factor is defined as the elastic modulus measured at a specific temperature divided by

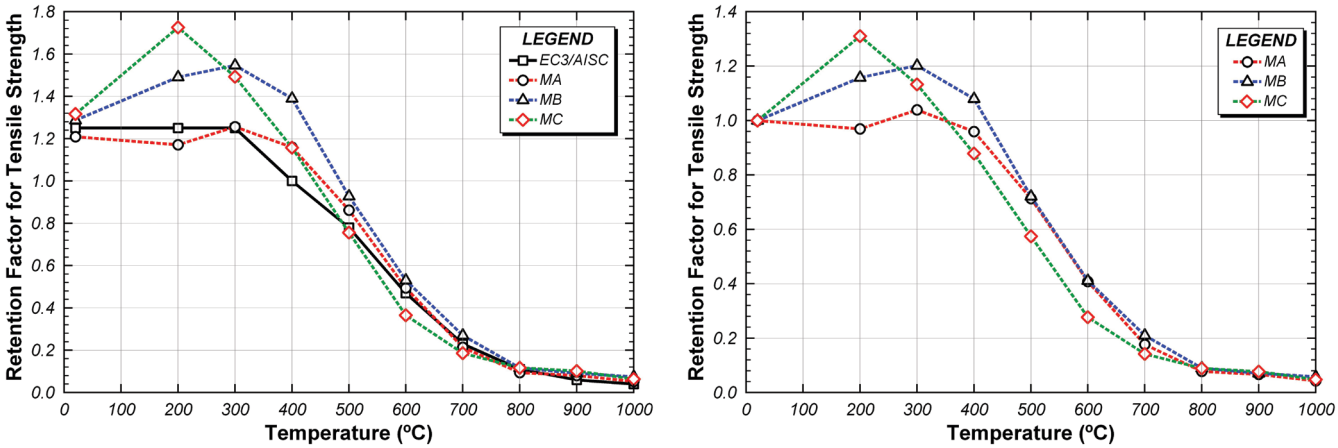

(a) Using ($f_{u,T}/f_{y,20°C}$) definition *(b) Using ($f_{u,T}/f_{u,20°C}$) definition*

Fig. 15. Tensile strength retention factors.

Table 4. Tensile Strength at Elevated Temperatures (ksi)										
Temperature (°C)	**20**	**200**	**300**	**400**	**500**	**600**	**700**	**800**	**900**	**1000**
MA	76.2	73.8	79.2	73.1	54.3	31.1	13.5	5.9	5.1	3.3
MB	66.2	76.6	79.5	71.5	47.7	27.2	13.9	5.9	4.7	3.9
MC	68.3	89.4	77.4	60.0	39.2	18.9	9.7	6.1	5.3	3.3

the elastic modulus at ambient temperature. Compared to Eurocode 3 (2006) and the AISC *Specification* (2010) in Figure 17, the experimental predictions of retention factors for elastic modulus show the same overall changing trend at elevated temperatures, albeit the reductions in the modulus values with temperature are less severe than predictions by Eurocode 3 and by AISC *Specification*. The elastic modulus data are more scattered among the three steel samples in comparison with the results shown earlier for the yield and tensile strength retention factors (referring to Figures 14 and 15), especially at temperatures at and above 600 °C. It is not clear whether this variability in elastic modulus values for different steel materials is an intrinsic material variability or, in fact, is an experimental error.

Proportional Limit

The proportional limit was determined by estimating the highest stress at which the curve in a stress-strain diagram is a straight line. At room temperature, the proportional limit is about the same as the yield stress. However, at high temperatures, proportional limits are usually significantly lower than yield stress. Figure 18 plots the calculated values of proportional limits for all steel materials at elevated temperatures, using stress-strain curves measured at a cross-head displacement rate of 0.01 in/min.

Retention factors for proportional limit at elevated temperatures are also calculated and compared with the corresponding ones in Eurocode 3 (2006) and in the AISC *Specification* (2010), as shown in Figure 19. In general, reasonable agreement can be found between experimental retention factors for proportional limit and those predicted by Eurocode 3 and by the AISC *Specification*.

It is important to note that compared with other mechanical properties considered here, the proportional limit shows a higher rate of reduction with increasing temperature (see Figures 14, 15, 17 and 19). This observation is important because the tangent modulus reduces rapidly after exceeding the proportional limit (Morovat et al., 2010, 2011). The rapid reduction of tangent modulus at elevated temperatures is particularly significant in stability related problems.

Elongation at Fracture

Figure 20 plots the elongation of the steel coupons with temperature, for coupons tested at a cross-head displacement rate of 0.01 in/min. As seen in this figure, the elongation for materials MA and MB is relatively constant for temperatures up to 500 °C; then shows a sharp increase up to 800 °C; and finally a sharp decrease at 900 °C, almost to its corresponding value at room temperature. The reason the maximum elongation occurs at 800 °C is most probably related to the

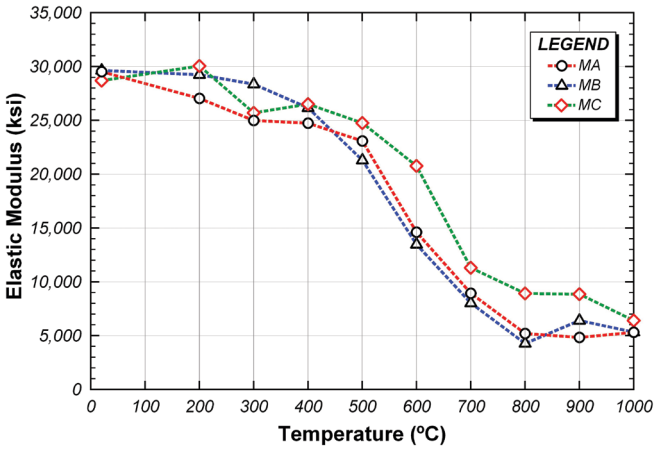

Fig. 16. Changes in elastic modulus with temperature.

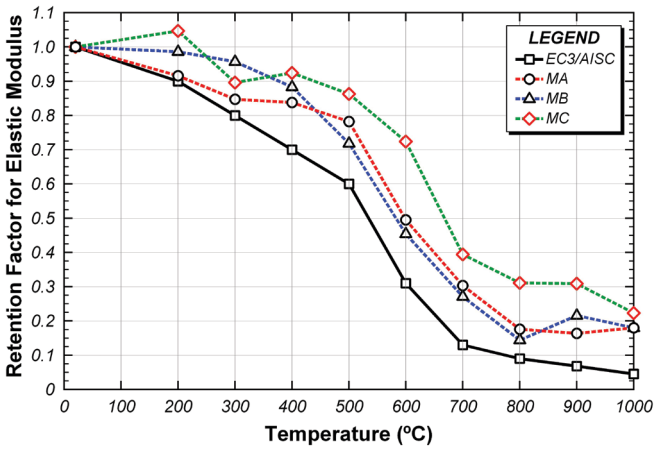

Fig. 17. Elastic modulus retention factors.

phase change around the eutectoid point for low-carbon steel at about 727 °C. Due to the phase change from ferrite (α-Fe) to austenite (γ-Fe), the elongation continuously increases up to the eutectoid point. In the case of material MC, the same trend can be observed, although with less variation that seen for materials MA and MB. The primary difference in the trend of elongation can be seen in the temperature range of 900 to 1000 °C, where material MB sees a drop in elongation while material MC experiences a rise in elongation.

Eurocode 3 (2006) does not provide retention factors for elongation, and as a result, no comparison with Eurocode 3 is provided here. However, Eurocode 3 provides equations for stress-strain curves where, irrespective of the temperature, a constant value of 20% is suggested for the elongation of steel at elevated temperatures. Stress-strain curves from Eurocode 3 will be discussed and compared with experimental results later in this paper.

Strain Corresponding to the Tensile Strength

Figure 21 plots the strain at which the tensile strength is developed, for coupons tested at a cross-head displacement rate of 0.01 in/min. As seen in this figure, the strain at the tensile strength shows a dramatic decrease with increasing temperature from 400 to 800 °C. For all three material samples, the lowest values of strain at the development of the tensile strength occurred at temperatures of 700 to 800 °C. At these temperatures, the strains at the development of the tensile strength were on the order of 1 to 2%, representing a very large reduction from the ambient temperature values, which were on the order of 16 to 18%. This trend further reinforces previous observations that the basic shape of the stress-strain curve for steel can be very different at elevated temperatures compared to ambient temperature.

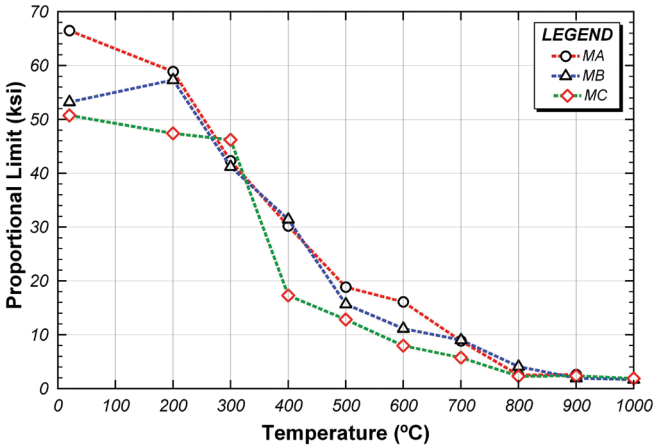

Fig. 18. Changes in proportional limit with temperature.

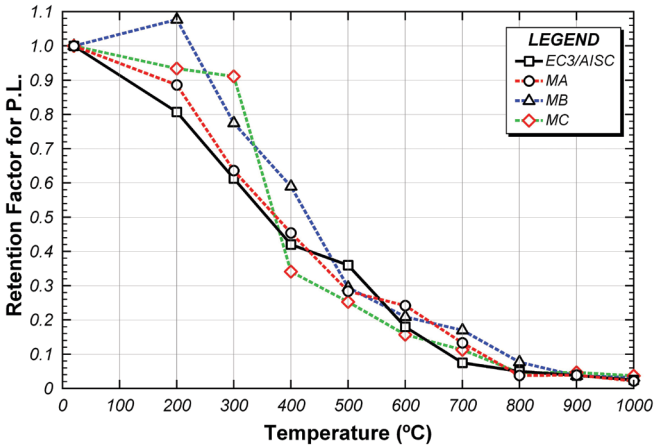

Fig. 19. Proportional limit retention factors.

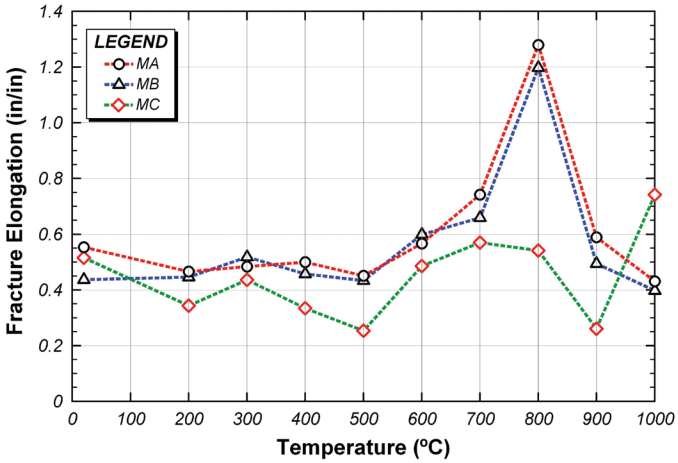

Fig. 20. Changes in elongation with temperature.

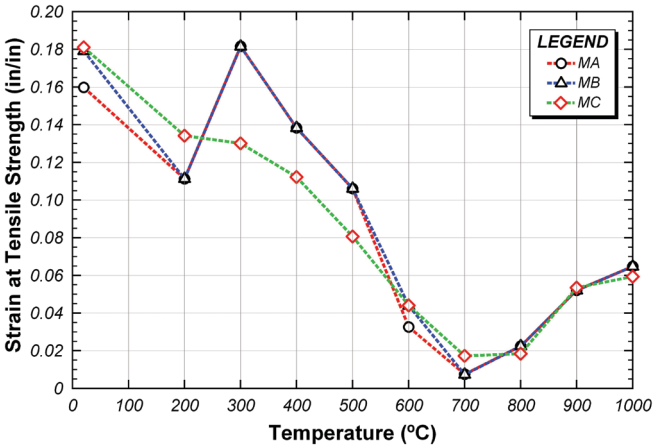

Fig. 21. Changes in strain corresponding to tensile strength with temperature.

Shape of Stress-Strain Curves

The use of advanced analysis methods, such as finite element analysis, to predict the response of steel structures to fire requires a more complete description of the elevated-temperature mechanical properties of steel, including data on the shape of the stress-strain curves at elevated temperatures. Eurocode 3 (2006) provides equations to predict the stress-strain curves for structural steel at elevated temperatures for use in advanced analysis. Generally speaking, these equations divide stress-strain curves into four sections and include both rising and descending portions of the stress-strain curves. In addition, these stress-strain curves do not include strain hardening, thereby assuming the yield and tensile strengths to be the same. Eurocode 3 has additional curves that include strain hardening at lower temperatures, although these curves are not considered in this paper.

In Figure 22, stress-strain curves from tests conducted at a cross-head displacement rate of 0.01 in./min are compared against the corresponding curves predicted by Eurocode 3 (2006) at several representative temperatures. It can be seen that at strains smaller than 15%, the Eurocode's simplified stress-strain relationships match the test data quite well. However, at strains larger than 15%, the Eurocode 3 model displays a faster stress drop and a smaller total elongation and ductility. It is also important to note that while the typical shapes of the stress-strain curves of Eurocode 3 are similar for all temperatures higher than 400 °C, the actual curves obtained from tests vary with temperature significantly. Furthermore, as can be seen in Figure 22, all the stress-strain curves terminate at 20% strain. In other words, in Eurocode 3, a temperature-independent value of 20% is considered for the final elongation of steel at elevated temperatures. This is not the case for experimental stress-strain curves, where final elongation changes significantly with temperature.

It should be noted that stress-strain curves presented in Figure 22 correspond to the tests conducted at the lower displacement rate (0.01 in./min). When the Eurocode 3 (2006) equations are compared with stress-strain curves from tests conducted at the higher displacement rate (0.1 in./min), the correlation is not as good as that seen in Figure 22.

INTERPRETATION OF HIGH-TEMPERATURE STRESS-STRAIN DATA

This section provides more in-depth discussion on two major aspects of the behavior of ASTM A992 steel at elevated temperatures that have direct implications in the design of steel structures for fire: definition of yield stress and treatment of time-dependent effects.

Definition of F_y for Use in Design Equations at Elevated Temperatures

As noted before in the discussion of retention factors for yield stress at elevated temperatures, different definitions of yield stress can result in significantly different values of yield stress, especially at temperatures below 600 °C. Three definitions were considered earlier for yield stress, corresponding to the stress at 0.2% offset strain, 0.5% total strain and 2% total strain. As shown earlier in Figure 13, for a test conducted at 400 °C, these three definitions resulted in yield stress values of 43.8, 45.8 and 57.5 ksi. Clearly, the definition adopted for yield stress has a very large impact on the resulting yield stress value. As also noted earlier, Eurocode 3 (2006) and the AISC *Specification* (2010) define the elevated-temperature yield stress (effective yield stress in Eurocode 3) as the stress at a total strain of 2%. A review of past test programs on the elevated-temperature properties of structural steel showed that a number of different definitions for yield stress were adopted by various authors (Kirby and

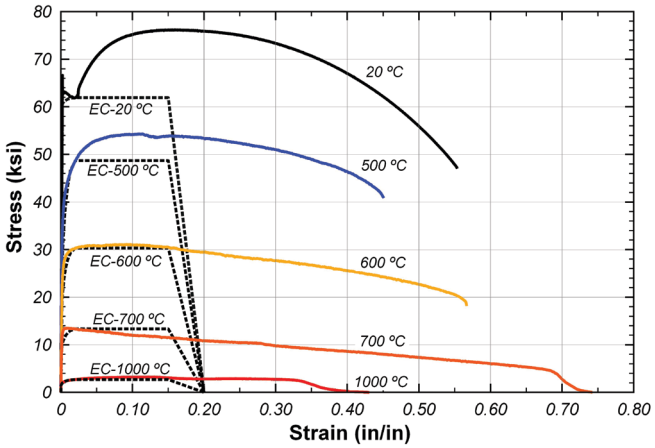

(a) Complete stress-strain curves

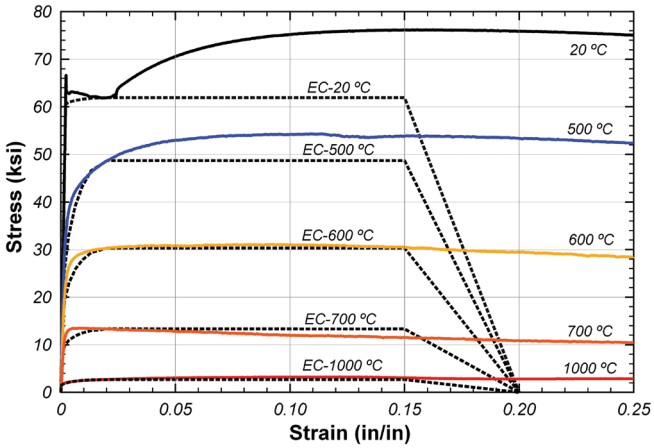

(b) Stress-strain curves up to 25% strain

Fig. 22. Experimental stress-strain curves compared to stress-strain curves from Eurocode 3 (2006).

Preston, 1988) and that at least some of the apparent variability in elevated-temperature yield stress values reported in the literature was due to variations in the definition of yield stress.

To consider the most appropriate definition of elevated-temperature yield stress in design, it is instructive to consider how yield stress values are used in calculations of member strength. In general, yield stress is used in computing member strength based on yield limit states and based on stability limit states. For yield limit states at ambient temperature, the value of yield stress is used to compute, for example, the plastic moment capacity of a wide-flange cross-section, $M_p = Z\ F_y$, the plastic shear capacity of a cross-section, $V_p = 0.6F_y\ A_{web}$, and the plastic axial capacity of a cross-section, $P_y = A\ F_y$. In these equations, Z is the plastic section modulus, A_{web} is the web area, A is the total cross-sectional area, and F_y is the minimum specified yield stress at ambient temperature (50 ksi for ASTM A992 steel, 36 ksi for ASTM A36 steel, etc.). When computing member strength at elevated temperatures for yield limit states, both Eurocode 3 (2006) and the AISC *Specification* (2010) use their own specific formulas for ambient temperature but replace F_y with $F_{y(T)}$, where $F_{y(T)}$ is the value of yield stress at temperature T. The value of $F_{y(T)}$ is determined by multiplying the ambient value of F_y by the yield stress retention factor for temperature T. Thus, the corresponding elevated-temperature cross-section strength values are simply $M_{p(T)} = ZF_{y(T)}$, $V_{p(T)} = 0.6\ F_{y(T)}\ A_{web}$, and $P_{y(T)} = \mathrm{A}\ F_{y(T)}$.

To better gauge the design implications of different definitions for the yield stress when computing elevated-temperature strength based on yield limit states, a simply supported beam was analyzed using finite element analysis at elevated temperatures using the stress-strain curves obtained in this testing program. The model is shown as insets in Figure 23 and consists of a 30-ft-long W18×60 beam with two equal concentrated, symmetrically applied loads. The model was developed on the finite element analysis program Abaqus (2011). The beam was analyzed at 400 °C and at 600 °C. For each temperature, the measured stress-strain curve for material MC was used as input to Abaqus.

Figure 23 shows the results of the Abaqus analysis. Analysis results are plotted as moment in the beam (computed as the applied load P multiplied by 120 in.) versus mid-span displacement. Results are plotted for 400 and 600 °C. Also shown in each plot is the computed plastic moment capacity of the beam, $M_{p(T)} = ZF_{y(T)}$. Three different values of $M_{p(T)}$ are shown on each plot, corresponding to three different definitions of $F_{y(T)}$. Thus, these plots provide a comparison of the estimated actual bending capacity of the beam based on Abaqus analysis, and the bending capacity as would be computed in a design calculation; that is, $M_{p(T)} = ZF_{y(T)}$. Among the three yield stress definitions, the value of $M_{p(T)}$ based on yield stress at 2% total strain appears to provide the best estimate of the bending capacity predicted by the Abaqus analysis. When this bending capacity is achieved, the predicted mid-span displacement of the 30-ft-long beam is about 25 to 30 in. for both temperatures. While this deflection is quite large, it can be argued that in an extreme fire scenario, such deflections may be considered acceptable, as long as the beam can safely support its load. On the other hand, if the design objective is to limit deflections of the beam in a fire scenario to relatively small values, perhaps to allow for easier repair, then adopting the 0.2% offset strain definition for yield stress may be more reasonable. For this example, if $M_{p(T)}$ is computed using the 0.2% offset definition of yield stress, the predicted deflection of the 30-ft-long beam is about 5 in. for both temperatures. Thus, the most appropriate definition of yield stress for calculating elevated-temperature member strength for yield limit states is a matter of judgment and structural performance requirements.

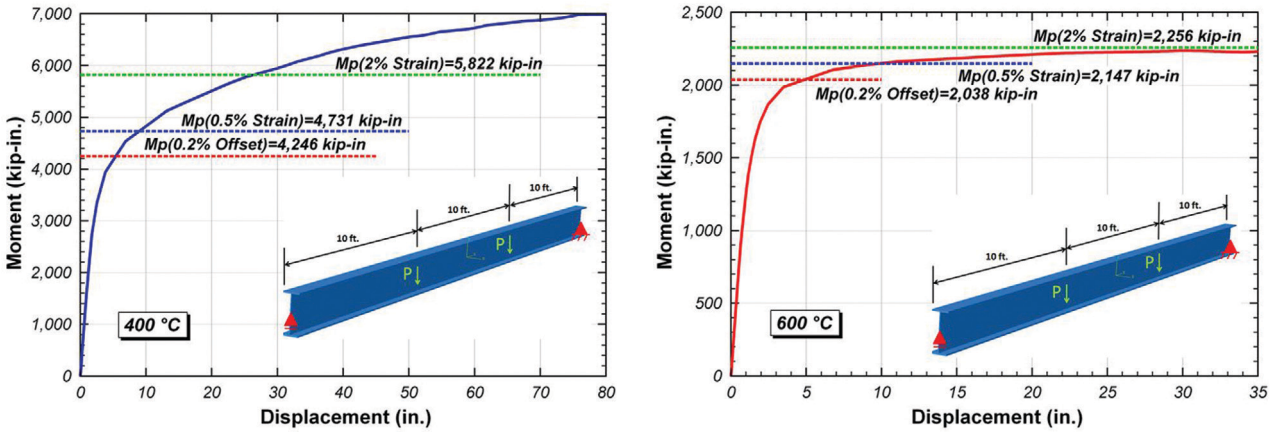

(a) Beam response at 400 °C

(b) Beam response at 600 °C

Fig. 23. The load-carrying capacity of a steel beam at elevated temperatures.

However, in the view of the authors, the definition of yield stress based on 2% total strain, as currently used in Eurocode 3 (2006) and the AISC *Specification* (2010), seems to provide a reasonable basis for design.

As noted earlier, values of yield stress are also used when computing member strength based on stability limit states (e.g., when computing column buckling capacity). Buckling capacity is more closely related to material stiffness than to material strength, and ambient-temperature formulas for column capacity depend on both E and F_y of the steel. However, to predict column capacity at elevated temperatures, it is not possible to use ambient-temperature formulas for column buckling and simply replace E and F_y at ambient with the corresponding values $E_{(T)}$ and $F_{y(T)}$ at the temperature of interest (Takagi and Deierlein, 2007; Ho, 2010). This is because of the highly nonlinear shape of the stress-strain diagram and the substantial difference between yield stress and proportional limit for steel at elevated temperatures. That is, the fundamental shape of the stress-strain diagram for steel at elevated temperatures is very different than the shape at ambient, and this difference has a large impact on buckling behavior. Thus, design formulas for buckling at elevated temperatures must consider values of modulus of elasticity, proportional limit, and yield stress at elevated temperatures, and the formulas must be calibrated or fit to either experimental or numerical predictions of column buckling capacity. Such a calibration can be done using any of the possible definitions of yield stress. For example, equations for flexural buckling of columns and lateral torsional buckling of beams at elevated temperatures provided in the AISC *Specification* (2010) use the value of yield stress at 2% total strain, based on calibration to numerical buckling predictions by Takagi and Deierlein (2007). Thus, when choosing a definition of yield stress at elevated temperatures for use in computing buckling capacities, any of the definitions of elevated-temperature yield stress can be used, as long as the buckling formula has been appropriately calibrated to the chosen definition of yield stress.

In summary, the definition adopted for the yield stress of steel at elevated temperatures can have a large impact on the value of yield stress, and in turn, can have a large impact on the member strength calculations. At present, Eurocode 3 (2006) and the AISC *Specification* (2010) define elevated-temperature yield stress as the stress at a total strain of 2%. It should be further noted that Eurocode 3 (2006) refers to the 2% total strain as the yield strain and the yield stress corresponding to the 2% total strain as the effective yield stress. Based on the previous discussion, this definition of yield stress appears to provide a reasonable basis for member strength calculations at elevated temperatures. Note that when the response of a steel structure to fire is determined using advanced analysis, such as by finite element analysis, the actual elevated-temperature stress-strain curve can be used in the analysis, and there is no particular need to define a yield stress. Finally, for the three samples of ASTM A992 steel tested in this research program, the yield stress retention factors based on the 2% total strain definition match reasonably well with the yield stress retention factors defined in Eurocode 3 (2006) and the AISC *Specification* (2010).

Time Effects on Stress-Strain Behavior of Steel at Elevated Temperatures

Time-dependent or creep effects can have significant impact on the behavior of structural steel at elevated temperatures (Morovat et al., 2012; Lee, 2012). In general, time-dependent effects can be explicitly accounted for by conducting specific material characterization tests at elevated temperatures. One common way to characterize time-dependent effects on the

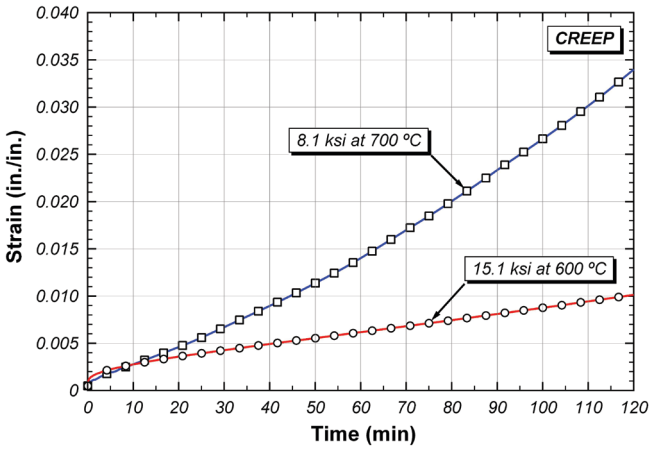

Fig. 24. Representative creep curves for material MC.

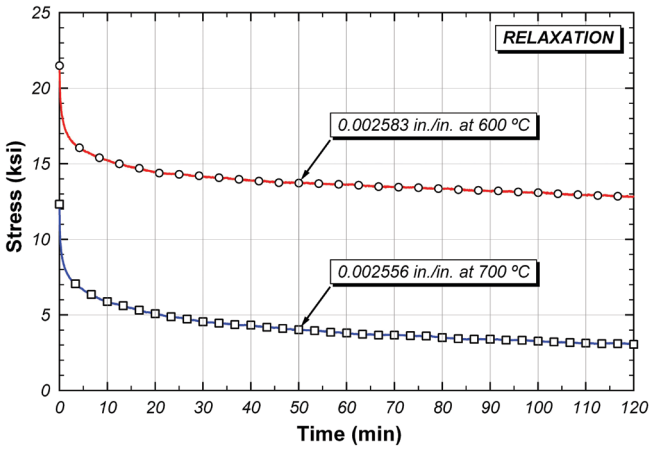

Fig. 25. Representative relaxation curves for material MC.

behavior of structural steel at high temperatures is to conduct creep tests, in which the steel coupons are subjected to constant stress and temperature and strain is measured as a function of time. Representative results of such tests, known as creep curves, for material MC are shown in Figure 24. Another common way to study the time-dependency of steel material behavior at high temperatures is to conduct relaxation tests, in which the steel coupons are subjected to constant strain and temperature, and stress is measured as a function of time. Sample results of such tests, known as stress relaxation curves, for material MC are shown in Figure 25.

Data like those shown in Figures 24 and 25 clearly show the significant time dependency of steel material behavior at elevated temperatures. As described earlier in this paper, an apparent difference between stress-strain predictions from steady-state and transient-state temperature tests is in the way they treat the rate- or time-dependent effects. In steady-state temperature tests, rate effects are considered using load or displacement rates, while in transient-state temperature tests, such effects are taken into account using heating rates. Stress-strain curves obtained at two different displacement rates and shown in Figure 9 are examples of how the rate-dependent effects are considered in the steady-state temperature tests. As mentioned previously, these curves clearly indicate the significance of rate or time effects on the stress-strain behavior of structural steel at elevated temperatures, especially at temperatures at or above 500 °C. What is even more significant about the stress-strain curves in Figure 9 is that they represent the complexities involved in interpreting the results of tensile tests at elevated temperatures for use in design. Another difficulty in choosing stress-strain curves most representatives of the structural steel behavior at high temperatures is that there is no clear basis on how to compare the results from steady-state and transient-state temperature tests at elevated temperatures.

Based on the preceding discussion, it seems that the interpretation of material test results in designing steel structures for fire safety should consider how the effect of creep should be treated in analysis. If creep is explicitly considered in the analysis using high-temperature creep models for structural steel (e.g. Harmathy, 1967; Fields and Fields, 1989; Lee, 2012; Morovat et al., 2012), the basic stress-strain curves should probably have the least amount of creep present in them, and testing at higher strain rates is perhaps more appropriate. On the other hand, for some design problems, considering creep in just a very approximate way may be acceptable, and the lower loading rates, which implicitly include a significant amount of creep, are perhaps more justifiable. Unfortunately, while some studies suggest testing rates at which creep becomes significant in tension tests at elevated temperatures (Cooke, 1988; Kirby and Preston, 1988; Outinen, 2006), it is not clear how fast tension tests should be performed so that they become time-independent or how slowly they should be run in order to include an appropriate amount of creep in the structural response analysis. Consequently, the interpretation of tensile stress-strain data at elevated temperatures is somewhat influenced by the treatment of rate effects and time effects. This is an area that merits additional research, particularly at high temperatures where time-dependent effects become more important.

CONCLUSIONS

Results of an experimental program on the mechanical properties of ASTM A992 structural steel at elevated temperatures have been presented along with testing techniques and procedures. Steady-state temperature tests were conducted on steel coupons in tension at temperatures up to 1000 °C. In addition to elevated-temperature mechanical properties in tension, Charpy V-Notch (CVN) impact values were obtained to evaluate energy absorption capacity at elevated temperatures.

As a result of the tension tests, full-range stress-strain curves at elevated temperatures were obtained. The effect of loading rates on the steel strength at high temperatures was also examined by comparing the results of tension tests conducted at the cross-head displacement rates of 0.01 in./min and 0.1 in./min. Further, static yielding behavior was investigated in this study. It is shown that the displacement rate has a large impact on the steel strength at elevated temperatures, especially at temperatures higher than 600 °C.

The yield stress, tensile strength, elastic modulus and proportional limit obtained from the tensile stress-strain curves at elevated temperatures were compared with values specified by Eurocode 3 (2006) and the AISC *Specification* (2010). The measured values of yield stress agree reasonably well with Eurocode 3 and the AISC *Specification*, when yield stress is defined as the stress at 2% total strain. Elevated-temperature values of tensile strength, modulus of elasticity and proportional limit measured in these tests also agree reasonably well with predictions in Eurocode 3 and in the AISC *Specification*.

The data collected in this testing program also showed that the definition adopted for the yield stress of steel at elevated temperatures can have a large impact on the value of yield stress, and in turn, can have a large impact on the member strength calculations. At present, Eurocode 3 (2006) and the AISC *Specification* (2010) define elevated-temperature yield stress as the stress at a total strain of 2%. Based on analysis and discussion provided in this paper, this definition of yield stress appears to provide a reasonable basis for member strength calculations at elevated temperatures. It should be emphasized, however, that the question of how to define yield stress of structural steel requires further analysis and discussion within the design community.

ACKNOWLEDGMENTS

The research reported herein was conducted as part of research projects on "Elevated Temperature Performance of Beam End Framing Connections," "Creep Buckling of Steel Columns Subjected to Fire" and "Elevated Temperature Performance of Shear Connectors for Composite Beams," all supported by the National Science Foundation (NSF awards 0700682, 0927819 and 1031099, respectively). Elevated temperature material tests were conducted using equipment procured through an NSF Major Research Instrumentation Grant (NSF award CMS-0521086, "Acquisition of a High-Temperature Testing Facility for Structural Components and Materials"). The support of the National Science Foundation and of former NSF Program Directors M.P. Singh and Douglas Foutch is gratefully acknowledged. The authors are also grateful to Gerdau-Ameristeel for donating materials for this research. The authors would especially like to thank Matthew Gomez of Gerdau-Ameristeel for his support of this research. Finally, special thanks are due to the technical staff at the Ferguson Structural Engineering Laboratory at the University of Texas at Austin for their extensive assistance with the this testing program. Any opinions, findings and conclusions or recommendations expressed in this paper are those of the authors and do not necessarily reflect the views of the National Science Foundation.

REFERENCES

Abaqus (2011), Abaqus Version 6.11 User's Manual, Dassault Systèmes Simulia Cor., Providence, RI.

AISC (2010), *Specification for Structural Steel Buildings*, Standard ANSI/AISC 360-10, American Institute of Steel Construction, Inc., Chicago, IL.

ASTM A370-12 (2012), *Standard Test Methods and Definitions for Mechanical Testing of Steel Products*, American Society for Testing and Materials, West Conshohocken, PA.

ASTM A992-11 (2011), *Standard Specification for Structural Steel Shapes*, American Society for Testing and Materials, West Conshohocken, PA.

ASTM E21-09 (2009), *Standard Test Methods for Elevated Temperature Tension Tests of Metallic Materials*, American Society for Testing and Materials, West Conshohocken, PA.

Beedle, L. and Tall, L. (1960), "Basic Column Strength," *Journal of the Structural Division*, ASCE, Vol. 86, No. 7, pp. 139–173.

Chen, J., and Young, B. (2006), "Stress-Strain Curves for Stainless Steel at Elevated Temperatures," *Engineering Structures*, Vol. 28, No. 2, pp. 229–239.

Cooke, G.M.E. (1988), "An Introduction to Mechanical Properties of Structural Steel at Elevated Temperatures," *Fire Safety Journal*, Vol. 13, No. 1, pp. 45–54.

DeFalco, F.D. (1974), "Investigation of the Compressive Response of Modern Structural Steels at Fire Load Temperatures," PhD Dissertation, Department of Civil Engineering, University of Connecticut.

Dieter, G.E. (1986), *Mechanical Metallurgy*, 3rd ed., McGraw-Hill, New York, NY.

Eurocode 3 (2006), *Design of Steel Structures. Part 1-2: General Rules.* Structural Fire design, EN 1993-1-2, European Committee for Standardization, CEN.

Fields, B.A. and Fields, R.J. (1989), "Elevated Temperature Deformation of Structural Steel," Report NISTIR 88-3899, National Institute of Standards and Technology, Gaithersburg, MD.

Fujimoto, M., Furumura, F., Ave, T. and Shinohara, Y. (1980), "Primary Creep of Structural Steel (SS41) at High Temperatures," *Trans. of Architectural Institute of Japan*, Vol. 296, pp. 145–157.

Fujimoto, M., Furumura, F. and Ave, T. (1981), "Primary Creep of Structural Steel (SM50A) at High Temperatures," *Trans. of Architectural Institute of Japan*, Vol. 306, pp. 148–156.

Harmathy, T.Z. (1967), "A Comprehensive Creep Model," *Journal of Basic Engineering, Transactions*, ASME, Vol. 89, No. 3, pp. 496–502.

Harmathy, T.Z. and Stanzak, W.W. (1970), "Elevated-Temperature Tensile and Creep Properties of Some Structural and Prestressing Steels," *Fire Test Performance,* ASTM STP 464, American Society for Testing and Materials, pp. 186–208.

Ho, C. (2010), "Analysis of Thermally Induced Forces in Steel Columns Subjected to Fire," MS Thesis, Department of Civil, Architectural and Environmental Engineering, University of Texas at Austin.

Hu, G., Morovat, M.A., Lee, J., Schell, E. and Engelhardt, M.D. (2009), "Elevated Temperature Properties of ASTM A992 Steel," *Proc. Structures Congress*, ASCE, Austin, April 30–May 2, 2009.

Humphreys, F.J. and Hatherly, M. (2004), *Recrystallization and Related Annealing Phenomena*, 2nd ed., Elsevier Science Ltd, Oxford.

Kirby, B.R. and Preston, R.R. (1988), "High Temperatures Properties of Hot-rolled Structural Steels for Use in Fire Engineering Design Studies," *Fire Safety Journal*, Vol. 13, No. 1, pp. 27–37.

Kelly, F.S. and Sha, W. (1999), "A Comparison of the Mechanical Properties of Fire-Resistant and S275 Structural Steels," *Journal of Constructional Steel Research*, Vol. 50, No. 3, pp. 223–233.

Lee, J. (2012), "Elevated Temperature Properties of Steel for Structural Fire Engineering Analysis," PhD Dissertation, Department of Civil, Architectural and Environmental Engineering, The University of Texas at Austin.

Li, G.Q., Jiang, S.C., Yin, Y.Z., Chen, K. and Li, M.F. (2003), "Experimental Studies on the Properties of Constructional Steels at Elevated Temperatures," *Journal of Structural Engineering*, ASCE, Vol. 129, No. 12, pp. 1717–1721.

Lie, T.T. (Ed.). (1992), *Structural Fire Engineering*, ASCE Manuals and Reports on Engineering Practice No. 78, American Society of Civil Engineers, New York, NY.

Luecke, W.E., McColskey, J.D., McCowan, C.N., Banovic, S.W., Fields, R.J., Foecke, T., Siewert, T.A. and Gayle, F.W. (2005), "Federal Building and Fire Safety Investigation of the World Trade Center Disaster—Mechanical Properties of Structural Steels," Report NCSTAR 1-3, National Institute of Standards and Technology, Gaithersburg, MD.

Morovat, M.A., Lee, J., Hu, G. and Engelhardt, M.D. (2010), "Tangent Modulus of ASTM A992 Steel at Elevated Temperatures." *Proc. Sixth International Conference on Structures in Fire* (SiF 10), Michigan State University, East Lansing, Michigan, June 2–4, 2010.

Morovat, M.A., Engelhardt, M.D., Taleff, E.M. and Helwig, T.A. (2011), "Importance of Time-Dependent Material Behavior in Predicting Strength of Steel Columns Exposed to Fire," *Applied Mechanics and Materials*, Vol. 82, pp. 350–355.

Morovat, M.A., Lee, J., Engelhardt, M.D., Taleff, E.M., Helwig, T.A. and Segrest, V.A. (2012), "Creep Properties of ASTM A992 Steel at Elevated Temperatures," *Advanced Materials Research*, Vols. 446–449, pp. 786–792.

Outinen, J. (2006), *Mechanical Properties of Structural Steel at Elevated Temperatures and After Cooling Down*, Helsinki University of Technology, Laboratory of Steel Structures, Finland.

Skinner, D.H. (1972), "Measurement of High Temperature Properties of Steel," BHP Melbourne Research Laboratories, Report MRL 6/10, The Broken Hill Proprietary Company Limited Australia.

SSRC (1987), *Technical Memorandum No. 8: Standard Methods and Definitions for Tests for Static Yield Stress*, Structural Stability Research Council.

Takagi, J. and Deierlein, G.G. (2007), "Strength Design Criteria for Steel Members at Elevated Temperatures," *Journal of Constructional Steel Research*, Vol. 63, pp. 1036–1050.

Twilt, L. and Both, C. (1991), *Stress-Strain Relationships of Structural Steel at Elevated Temperatures: Analysis of Various Options & European Proposal*, SA 112 Part F: Mechanical Properties, TNO Building and Construction Research, Delft, The Netherlands.

United States Steel (1972), *Steels for Elevated Temperature Service*, United States Steel Corporation, Pittsburgh, PA.